Title
Coordinate suppression of B cell lymphoma by PTEN and SHIP phosphatases

Journal
Journal of Experimental Medicine, 207(11)

ISSN
0022-1007

Authors
Miletic, Ana V
Anzelon-Mills, Amy N
Mills, David M
et al.

Publication Date
2010-10-25

DOI
10.1084/jem.20091962

Peer reviewed

Coordinate suppression of B cell lymphoma by PTEN and SHIP phosphatases

Ana V. Miletic,[1] Amy N. Anzelon-Mills,[1] David M. Mills,[1] Sidne A. Omori,[1] Irene M. Pedersen,[2,3] Dong-Mi Shin,[4] Jeffrey V. Ravetch,[6] Silvia Bolland,[5] Herbert C. Morse III,[4] and Robert C. Rickert[1]

[1]Program of Inflammatory Disease Research, Infectious and Inflammatory Disease Center, Cancer Center, Sanford-Burnham Medical Research Institute, La Jolla, CA 92037
[2]Section of Molecular Biology, Division of Biological Sciences, and [3]University of California San Diego Cancer Center, University of California San Diego, La Jolla, CA 92093
[4]Laboratory of Immunopathology and [5]Laboratory of Immunogenetics, National Institute of Allergy and Infectious Diseases, National Institutes of Health, Rockville, MD 20852
[6]Laboratory of Molecular Genetics and Immunology, The Rockefeller University, New York, NY 10065

The inositol phosphatases phosphatase and tensin homologue (PTEN) and Src homology 2 domain–containing inositol phosphatase (SHIP) negatively regulate phosphatidylinositol-3-kinase (PI3K)–mediated growth, survival, and proliferation of hematopoietic cells. Although deletion of PTEN in mouse T cells results in lethal T cell lymphomas, we find that animals lacking PTEN or SHIP in B cells show no evidence of malignancy. However, concomitant deletion of PTEN and SHIP (bPTEN/SHIP$^{-/-}$) results in spontaneous and lethal mature B cell neoplasms consistent with marginal zone lymphoma or, less frequently, follicular or centroblastic lymphoma. bPTEN/SHIP$^{-/-}$ B cells exhibit enhanced survival and express more MCL1 and less Bim. These cells also express low amounts of p27^{kip1} and high amounts of cyclin D3 and thus appear poised to undergo proliferative expansion. Unlike normal B cells, bPTEN/SHIP$^{-/-}$ B cells proliferate to the prosurvival factor B cell activating factor (BAFF). Interestingly, although BAFF availability may promote lymphoma progression, we demonstrate that BAFF is not required for the expansion of transferred bPTEN/SHIP$^{-/-}$ B cells. This study reveals that PTEN and SHIP act cooperatively to suppress B cell lymphoma and provides the first direct evidence that SHIP is a tumor suppressor. As such, assessment of both PTEN and SHIP function are relevant to understanding the etiology of human B cell malignancies that exhibit augmented activation of the PI3K pathway.

CORRESPONDENCE
Robert C. Rickert:
robert@sanfordburnham.org

Abbreviations used: APRIL, a proliferation-inducing ligand; BAFF, B cell activating factor; BCR, B cell receptor; DLBCL, diffuse large B cell lymphoma; FL, follicular B cell lymphoma; GC, germinal center; MCL, mantle cell lymphoma; MZ, marginal zone; MZL, MZ lymphoma; PBL, peripheral blood lymphocyte; PI3K, phosphatidylinositol-3-kinase; PIP_3, phosphatidylinositol-(3,4,5)-trisphosphate; PTEN, phosphatase and tensin homologue; SHIP, Src homology 2 domain–containing inositol phosphatase.

Phosphatidylinositol-3-kinase (PI3K) is activated downstream of numerous receptors and catalyzes the conversion of membrane phosphatidylinositol-(4,5)-bisphosphate ($PI_{4,5}P_2$) to phosphatidylinositol-(3,4,5)-trisphosphate (PIP_3). PIP_3 acts as a second messenger, recruiting to the plasma membrane pleckstrin homology domain–containing adaptors and kinases such as PDK1, Akt, PLC-γ, Tec family kinases, and DOK, which then further modulate downstream signaling (Cully et al., 2006). Subsequent activation or inactivation of cytosolic and nuclear targets, including SGK, mTOR, PP2A, FOXO, and cyclins D and E, mediates diverse cellular responses such as survival, proliferation, migration, adhesion, and differentiation (Cully et al., 2006). In B cells, attenuated PI3K signaling impairs B cell survival and selection, leading to diminished numbers of peritoneal B-1 cells, splenic marginal zone (MZ) B cells, and germinal center (GC) B cells, as well as a general reduction in mature recirculating B cells (Donahue and Fruman, 2004).

The action of PI3K is antagonized by two lipid phosphatases: the 3′-inositol phosphatase, phosphatase and tensin homologue (PTEN), and the 5′-inositol phosphatase Src homology 2 (SH2) domain–containing inositol phosphatase (SHIP).

A.V. Miletic, A.N. Anzelon-Mills, and D.M. Mills contributed equally to this paper.

The Rockefeller University Press $30.00
J. Exp. Med. Vol. 207 No. 11 2407-2420
www.jem.org/cgi/doi/10.1084/jem.20091962

The Journal of Experimental Medicine

Although both PTEN and SHIP hydrolyze PIP_3, the generation of their distinct lipid products, $PI_{4,5}P_2$ and $PI_{3,4}P_2$, respectively, likely confers specificity in effector recruitment to the plasma membrane. PTEN is a ubiquitously expressed and highly active enzyme that regulates basal and induced PIP_3 levels via dynamic interactions with the plasma membrane (Vazquez and Devreotes, 2006). In contrast, plasma membrane recruitment of hematopoietically restricted SHIP requires binding of its SH2 domain to proteins bearing specific phosphotyrosine motifs (Rohrschneider et al., 2000). In B cells, SHIP is recruited to the negative regulatory Fcγ receptor II-B, where it regulates signals induced by immune-complexed antigen. SHIP also attenuates autonomous B cell receptor (BCR) signaling via an unknown mechanism (Brauweiler et al., 2000b). The restricted versus expansive roles of SHIP and PTEN, respectively, are supported by in vivo studies of mice lacking SHIP and PTEN, individually, in B cells. In $SHIP^{-/-}$ mice, the peripheral B cell compartment is reduced whereas BCR-induced proliferation is enhanced (Liu et al., 1998; Brauweiler et al., 2000a; Helgason et al., 2000). PTEN-deficient B cells exhibit preferential differentiation into MZ or B-1 B cells and are hyperresponsive to extracellular stimuli (Anzelon et al., 2003; Suzuki et al., 2003). *PTEN* is the second most frequently mutated gene documented in human cancers (after the tumor suppressor *TP53*), and activation of the PI3K signaling pathway has been implicated in B cell neoplasia (Barragán et al., 2002; Cuní et al., 2004; Smith et al., 2005; Rudelius et al., 2006; Uddin et al., 2006). Nonetheless, *PTEN* gene mutations are surprisingly infrequent in human B cell malignancies (Sakai et al., 1998; Butler et al., 1999). Furthermore, although conditional deletion of *Pten* in mouse T lymphocytes leads to lethal T cell lymphomas, inactivation of *Pten* in B cells is not a transforming event (Suzuki et al., 2001, 2003; Anzelon et al., 2003). Thus, we hypothesized that the potential for PI3K-dependent B cell transformation remains suppressed in the absence of PTEN as a result of the activity of SHIP.

In this paper, we provide strong support for this hypothesis, showing that mice lacking expression of PTEN and SHIP in B cells ($bPTEN/SHIP^{-/-}$) develop lethal B cell lymphomas with similarities to human mature B cell lymphomas. $bPTEN/SHIP^{-/-}$ B cells exhibit enhanced PI3K signaling downstream of both BCR and cytokine receptors and an acquired mitogenic response to the survival factor B cell activating factor (BAFF). Analysis of cell cycle regulators suggests that the BCR and BAFF-R synergize to promote lymphoma progression. Together, these data represent the first demonstration of SHIP as a tumor suppressor. As such, assessment of both PTEN and SHIP function is relevant to understanding the etiology of B cell malignancies, such as diffuse large B cell lymphoma (DLBCL) and mantle cell lymphoma (MCL), which present augmented activation of the PI3K pathway (Rudelius et al., 2006; Uddin et al., 2006).

RESULTS

Deletion of *Pten* and *Ship* in B cells results in lethal disease characterized by splenomegaly, B cell expansion, and disrupted splenic architecture

Although deletion of *Pten* in mouse T cells results in lethal T cell lymphomas (Suzuki et al., 2001), animals lacking *Pten* in B cells ($bPTEN^{-/-}$) show no evidence of malignancy (Anzelon et al., 2003). Similarly, there are no reports of malignancies in mice lacking SHIP in B cells. To determine if PTEN and SHIP coordinately suppress B cell transformation, we generated mice with a B cell–specific deletion of both *Pten* and *Ship* ($bPTEN/SHIP^{-/-}$) by mating $bPTEN^{-/-}$ mice (Anzelon et al., 2003) with a novel strain of mice lacking SHIP only in B cells ($bSHIP^{-/-}$; see Materials and methods; Fig. S1 A). As early as 4 mo of age, $bPTEN/SHIP^{-/-}$ (but not $bPTEN^{-/-}$, $bSHIP^{-/-}$, or $bPTEN/SHIP^{+/-}$) mice exhibited lethargy, weight loss (Fig. 1 A), hunched posture, ruffled fur, and splenomegaly (Fig. 1, A and B). Severe morbidity and death occurred in all $bPTEN/SHIP^{-/-}$ animals by 1 yr of age (Fig. 1 C and not depicted). In contrast, WT, $bPTEN^{-/-}$, and $bSHIP^{-/-}$ controls did not develop splenomegaly and failed to display any signs of disease noted in $bPTEN/SHIP^{-/-}$ mice (Fig. 1, B and C). As compared with spleens of control animals, spleens of aged $bPTEN/SHIP^{-/-}$ mice (>6 mo of age) displayed an expansion of $CD19^+$ B cells, resulting in enlarged white pulp areas that often infiltrated and compressed the red pulp (Fig. 1, D and E; and not depicted). Notably, tissues containing the expanded B cell population also displayed an expansion of $CD11b^+$ myeloid cells (Fig. 1 E and not depicted). Concurrent with disease onset, $bPTEN/SHIP^{-/-}$ B cells and myeloid cells were found in liver and lung and, less frequently, kidney infiltrates and often formed visible masses in nonlymphoid tissues (Fig. 1 F). Thus, unlike loss of either PTEN or SHIP alone, loss of both PTEN and SHIP in B cells results in an aggressive and fatal disease associated with immune cell expansion.

$bPTEN/SHIP^{-/-}$ B cells acquire a surface phenotype consistent with B cell lymphoma

To determine whether the disease observed in $bPTEN/SHIP^{-/-}$ mice represents a lymphoproliferative disease or a neoplastic disorder, we examined the phenotypes of peripheral B cells in WT, $bPTEN^{-/-}$, $bSHIP^{-/-}$, and $bPTEN/SHIP^{-/-}$ animals. Flow cytometric analyses of peripheral blood lymphocytes (PBL) showed a reduction in the frequency of B cells in asymptomatic $bPTEN/SHIP^{-/-}$ mice (Fig. 2 A, pre, ≤6 mo) as compared with WT, $bPTEN^{-/-}$, or $bSHIP^{-/-}$ mice (Fig. 2 A), perhaps as a result of retention of B cells in the lymphoid tissues. $bPTEN/SHIP^{-/-}$ animals older than 6 mo had a threefold increase in the percentage of recirculating B cells in the blood, concurrent with the onset of disease (Fig. 2 A). Notably, the percentage of $CD19^+$ B cells in $bPTEN/SHIP^{-/-}$ animals was comparable to that of WT, $bPTEN^{-/-}$, and $bSHIP^{-/-}$ mice, even in the blood of diseased $bPTEN/SHIP^{-/-}$ mice (Fig. 2 B). However, in the latter group, the associated severe splenomegaly likely indicates a parallel expansion or recruitment of non–B cells into the spleen. Moreover, although diseased $bPTEN/SHIP^{-/-}$

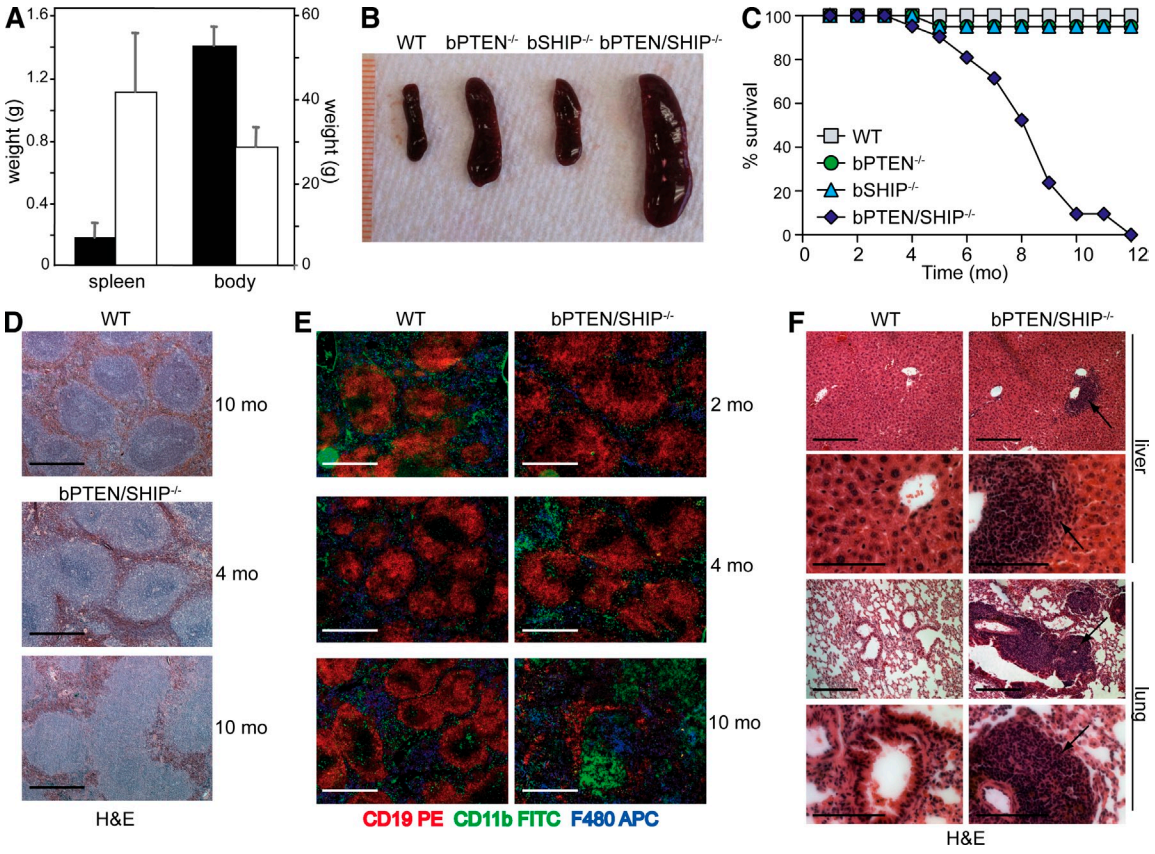

Figure 1. bPTEN/SHIP$^{-/-}$ mice develop a lethal disease characterized by weight loss, splenomegaly, and altered splenic architecture. (A) Spleen (left axis) and body (right axis) weight (grams) of WT (black bar) and bPTEN/SHIP$^{-/-}$ (white bar) mice between 7 and 12 mo of age (n = 7). Error bars represent SD of spleen and body weights of WT or bPTEN/SHIP$^{-/-}$ mice shown. (B) Representative photograph of spleens from WT (12 mo), bPTEN$^{-/-}$ (12 mo), bSHIP$^{-/-}$ (12 mo), and bPTEN/SHIP$^{-/-}$ (8 mo) mice. Image is representative of n > 25 mice of each genotype. (C) Survival of WT (n = 20), bPTEN$^{-/-}$ (n = 15), bSHIP$^{-/-}$ (n = 15), and bPTEN/SHIP$^{-/-}$ (n = 20) mice monitored for 1 yr. (D) Hemotoxylin/eosin (H&E) staining of microsections from paraffin-embedded spleens. The age of mice shown was 4 or 10 mo, as indicated. Pictures are representative of >40 mice of each genotype. Magnification shown is with a 5× objective. Bars, 500 µm. (E) Immunofluorescence of spleens of WT and bPTEN/SHIP$^{-/-}$ mice of indicated ages stained with α-CD19-PE (red), α-CD11b-FITC (green), and F4/80-APC (blue). Magnification shown is 5×. Bars, 500 µm. (F) H&E-stained sections from paraffin-embedded liver (top) and lung (bottom) of WT and bPTEN/SHIP$^{-/-}$ mice. Arrows indicate white blood cell infiltrates. Results are representative of >20 WT and bPTEN/SHIP$^{-/-}$ mice >6 mo of age. Magnification shown is with a 5× objective (first and third rows) or 40× objective (second and fourth rows). Scale bars: (5×) 500 µm; (40×) 100 µm.

mice had hematocrits and hemoglobin values comparable to those of age-matched WT controls, peripheral blood smears revealed lymphocytes that resembled lymphoma cells based on cell size and nuclear features (unpublished data).

Flow cytometric analyses of recirculating CD19^{+} bPTEN/SHIP$^{-/-}$ B cells showed that they were larger than B cells from WT, bPTEN$^{-/-}$, or bSHIP$^{-/-}$ mice, as indicated by forward light scatter (Fig. 2 C). bPTEN/SHIP$^{-/-}$ B cells were predominantly B220$^{low/-}$IgM$^{+/low}$IgD^{-}CD11b^{+}CD5$^{+/low}$CD43^{+}CD21$^{-/low}$CD23^{-} (Fig. 2, B and C) but did not express markers characteristic of T cells (CD3, CD4, and CD8) or markers of dendritic cells (CD11c), granulocytes (Gr1), or macrophages/myeloid cells (F4/80; not depicted). In asymptomatic prelymphoma mice, splenic B cells exhibited bimodal expression of some markers, indicating the presence of normal and altered B cell populations (Fig. 2 C). By comparison, splenic B cells and B cells present in liver masses of diseased bPTEN/SHIP$^{-/-}$ mice shared an altered yet uniform phenotype, suggesting that bPTEN/SHIP$^{-/-}$ B cells found in nonlymphoid organs had metastasized from secondary lymphoid tissues (Fig. 2 C). The phenotype of bPTEN/SHIP$^{-/-}$ B cells was similar to that of B1a B cells that predominate in the peritoneal and pleural cavities of WT mice (Hardy et al., 2006) but was quite distinct from that of normal follicular, MZ, GC, or memory B cells. Importantly, however, most documented mouse B cell lymphomas, whether derived from MZ or GC B cells, are CD5^{low}, and a significant proportion also express CD11b (Fig. 2 C; Morse et al., 2002). Collectively, the surface phenotype and increased size of bPTEN/SHIP$^{-/-}$ B cells is consistent with B cell neoplasia.

PTEN/SHIP$^{-/-}$ B cells are oligoclonal and transfer disease

The majority of histologically defined mouse lymphomas are monoclonal or oligoclonal, as demonstrated by Southern blot

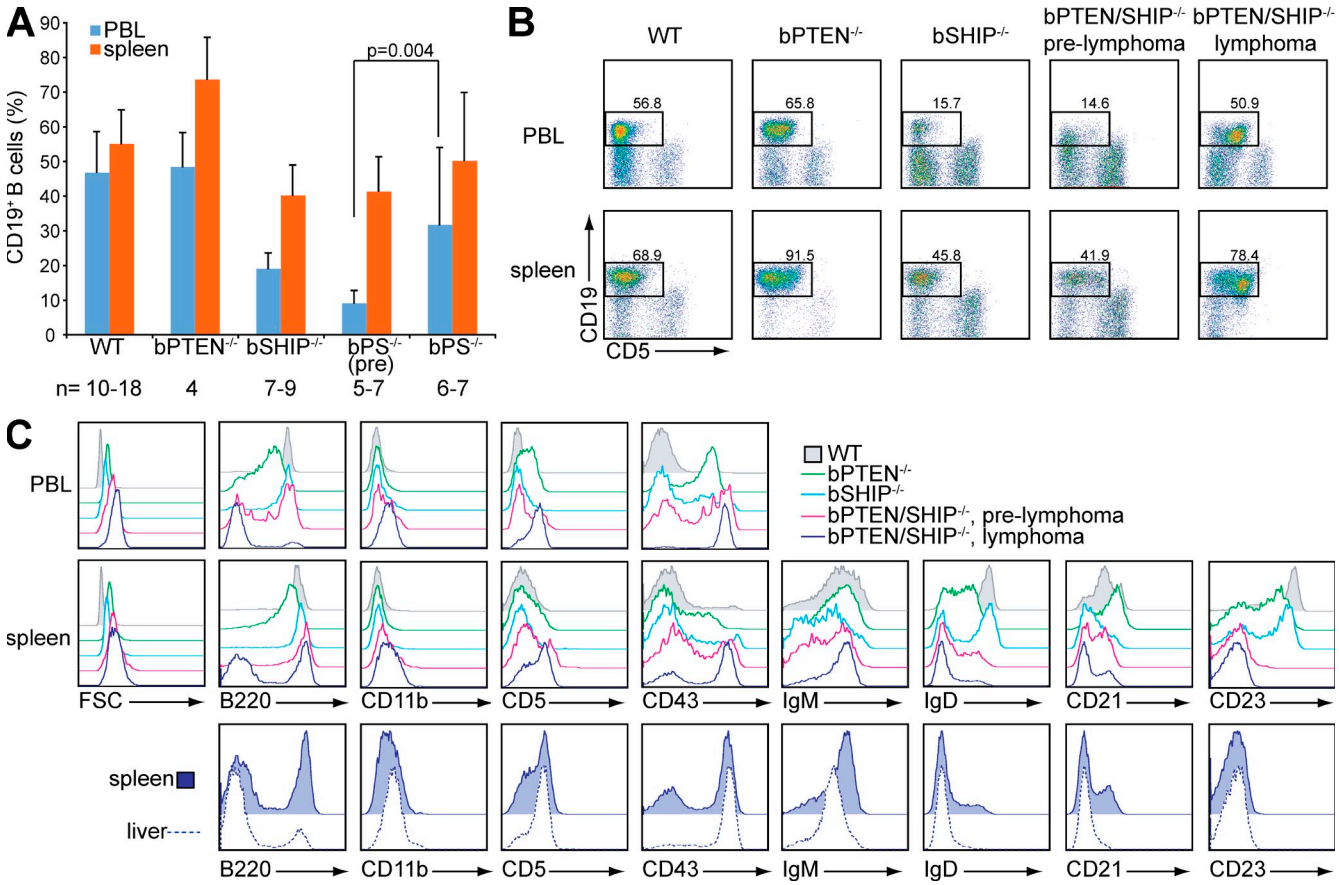

Figure 2. bPTEN/SHIP$^{-/-}$ B cells display a surface phenotype consistent with B cell lymphoma. (A) Percentage of CD19$^+$ leukocytes in peripheral blood (PBL) and spleen of indicated mice, as determined by flow cytometry. pre = prelymphoma; bPS = bPTEN/SHIP$^{-/-}$. P-value was determined by two-tailed Student's *t* test. Error bars represent SD of percentages of CD19$^+$ B cells in blood or spleens of mice shown. (B) Flow cytometric analysis of PBL or spleen comparing expression of CD19 versus CD5. Numbers above gates indicate the percentage of CD19$^+$ B cells in PBL or spleen, as indicated. (C) Flow cytometric analysis of CD19$^+$ cells in PBL or single cell suspensions of spleen (top) using antibodies against cell surface markers, as indicated. The bottom shows a comparison of liver metastases and spleen of a diseased bPTEN/SHIP$^{-/-}$ mouse. All histograms show gated CD19$^+$ cells. All flow cytometry data are representative of five independent age-matched cohorts. WT, $n = 10$; bPTEN$^{-/-}$, $n = 4$; bSHIP$^{-/-}$, $n = 9$; bPTEN/SHIP$^{-/-}$ pre, $n = 5$; bPTEN/SHIP$^{-/-}$, $n = 6$.

analysis of *Ig heavy chain* (*IgH*) *J* gene organization or by PCR analysis of *IgH V* gene usage (Morse et al., 2002). Thus, to further distinguish between neoplastic and lymphoproliferative disease, genomic DNA from splenic B cells of age-matched WT and bPTEN/SHIP$^{-/-}$ mice was analyzed by Southern blotting for clonal rearrangements at the *IgH* locus using the J_H-specific probe *pJ11* (Stall et al., 1988). Numerous J_H rearrangements were detected in genomic DNA from B cells of WT and asymptomatic (prelymphoma) bPTEN/SHIP$^{-/-}$ mice (Fig. 3 A), indicative of a polyclonal B cell pool. In striking contrast, distinct nongermline bands were identified in DNA from several diseased (lymphoma) bPTEN/SHIP$^{-/-}$ mice, revealing the presence of clonal B cell outgrowths (Fig. 3 A). PCR analyses using V_H1- and V_H5-specific 5′ and shared 3′ J_H primers were used to determine if B cells present in nonlymphoid tissues and spleen were of common origin in individual mice (Fig. 3 B). In several cases, the same dominant rearrangement was observed in B cells isolated from several tissues within the same animal, indicating that the same clones had disseminated from lymphoid to nonlymphoid organs in diseased bPTEN/SHIP$^{-/-}$ mice (Fig. 3 B).

Mouse B lymphoma cells differ from untransformed WT B cells in their capacity to expand and propagate disease after transfer into immunocompromised hosts. To determine if bPTEN/SHIP$^{-/-}$ B cells would transfer disease, WT or bPTEN/SHIP$^{-/-}$ B cells were transferred intravenously into T cell–deficient (TCR-βδ$^{-/-}$) recipients, and the presence of transferred cells was monitored in peripheral blood at regular intervals. Consistent with their designation as transformed cells, bPTEN/SHIP$^{-/-}$ B cells expanded after adoptive transfer into TCR-βδ$^{-/-}$ recipients, whereas WT B cells failed to persist (Fig. 4, A and B).

By 3 mo after transfer, CD19$^+$B220^{low}CD5$^+$CD11b$^+$ B cells represented 60–70% of peripheral blood B cells in recipients that received bPTEN/SHIP$^{-/-}$ B cells (Fig. 4, B and C). In contrast, WT B cells neither survived nor expanded after transfer (Fig. 4, B and C). Examination of IgH usage in B cells

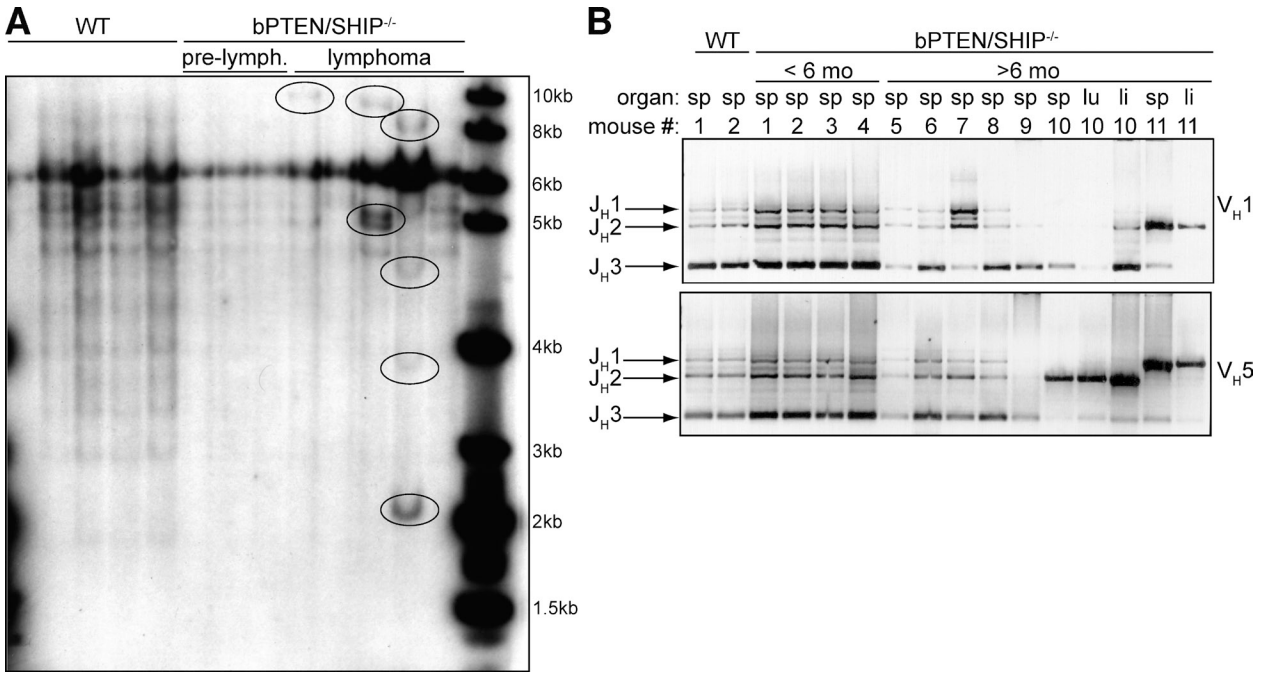

Figure 3. bPTEN/SHIP$^{-/-}$ B cells have oligoclonal Ig repertoires. (A) Rearrangements of the heavy chain of WT and bPTEN/SHIP$^{-/-}$ B cells were detected using the *pJ11* probe, which preferentially detects rearrangements to J_H1, J_H2, and J_H3. All mice were >6 mo of age and B cells were isolated from spleen. Pre-lymph. = prelymphoma. Clonal rearrangements are indicated by ellipses. Each lane represents an individual mouse. (B) PCR analysis of Ig *V-DJ$_H$* recombination using degenerate 5′ primers specific for either the distal *J558* (V_H1) or the proximal *7183* (V_H5) family and a common 3′ J_H4 primer on DNA from spleen (sp), liver (li), and/or lung (lu) from WT or bPTEN/SHIP$^{-/-}$ mice. Arrows indicate amplified *V-DJ$_H$1*, *V-DJ$_H$2*, and *V-DJ$_H$3* segment recombinations (1.3, 0.95, and 0.4 kb, respectively). Representative samples are shown for WT and young (<6 mo) and old (>6 mo) bPTEN/SHIP$^{-/-}$ mice.

transferred into TCR-βδ$^{-/-}$ recipients showed that all WT B cells (before and after transfer) showed a diverse polyclonal IgH repertoire (Fig. S2). Several TCR-βδ$^{-/-}$ recipient animals that received bPTEN/SHIP$^{-/-}$ B cells showed expansion of the same clones as the original transferred B cells, whereas others showed an expansion of unique clones that may not have been well represented in the original transferred population but expanded after transfer (Fig. S2). Additionally, 2–5 mo after adoptive transfer, recipients of bPTEN/SHIP$^{-/-}$ B cells exhibited signs of disease similar to those observed in unmanipulated bPTEN/SHIP$^{-/-}$ mice (Fig. 4 D) and, at necropsy, were found to have extensive cellular infiltrations of lungs, livers, and other nonlymphoid tissues (not depicted). The combined evidence of cell surface phenotype, clonality, and ability to transfer disease indicates that bPTEN/SHIP$^{-/-}$ mice develop B cell neoplasia rather than a B cell proliferative disease.

BAFF is mitogenic for bPTEN/SHIP$^{-/-}$ lymphoma cells

Similar to B cells from healthy mice, most explanted lymphoma cells generally do not replicate spontaneously ex vivo (despite the aggressive nature of most lymphomas in vivo), indicating that environmental stimuli are required for continued growth. In addition, however, mature B cells require tonic signaling via the BCR for maintenance and survival (Lam et al., 1997; Kraus et al., 2004). To understand which signals may contribute to the development of lymphomas in bPTEN/SHIP$^{-/-}$ mice, we first examined the in vitro proliferative responses of B cells lacking PTEN and/or SHIP to BCR stimulation. Consistent with previous results, bPTEN$^{-/-}$ and bSHIP$^{-/-}$ B cells proliferated robustly upon ligation of the BCR with anti-IgM F(ab')$_2$ fragments (Helgason et al., 2000; Anzelon et al., 2003; Suzuki et al., 2003). Intriguingly, however, bPTEN/SHIP$^{-/-}$ B cells were less responsive than bPTEN$^{-/-}$, bSHIP$^{-/-}$, or WT B cells (Fig. 5 A). Notably, bPTEN/SHIP$^{-/-}$ B cells were not generally refractory to proliferative stimuli, as they showed robust proliferative response to LPS or anti-CD40 that exceeded those of WT B cells and were comparable to those of bPTEN$^{-/-}$ B cells (Fig. S3). Because the adoptive transfer studies indicated that T cells or T cell–derived factors were not required for lymphomagenesis, we considered a role for BAFF, as it is broadly available in vivo and critical for B cell survival (Mackay and Schneider, 2009). The addition of BAFF to anti-IgM–stimulated cells enhanced proliferation in B cells from WT, bPTEN$^{-/-}$, bSHIP$^{-/-}$, and bPTEN/SHIP$^{-/-}$ mice (Fig. 5 A). Strikingly, treatment with BAFF alone induced proliferation of bPTEN/SHIP$^{-/-}$ but not of WT, bPTEN$^{-/-}$, or bSHIP$^{-/-}$ B cells (Fig. 5 A). Proliferation of bPTEN/SHIP$^{-/-}$ B cells to BAFF was unique, as treatment with the related cytokine, a proliferation-inducing ligand (APRIL), failed to induce a proliferative response (Fig. 5 A).

To examine how BCR ligation and BAFF stimulation promote cell cycle entry in bPTEN/SHIP$^{-/-}$ B cells, expression levels of p27^{kip1} and cyclin D3 were examined. The inability

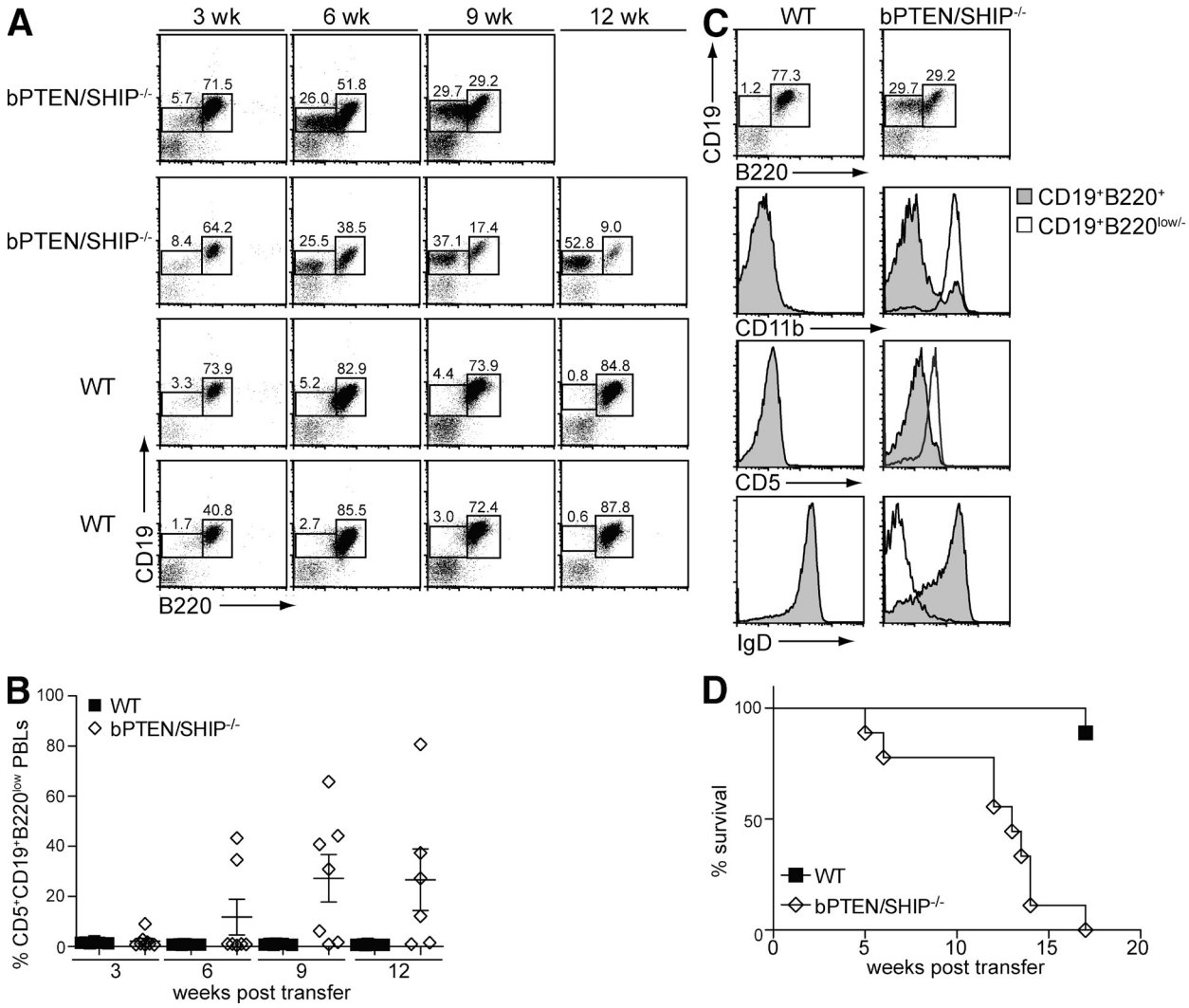

Figure 4. bPTEN/SHIP$^{-/-}$ B cells induce disease upon transfer into TCR-βδ$^{-/-}$ recipients. (A) bPTEN/SHIP$^{-/-}$ or WT splenic B cells from age-matched mice were transferred intravenously into TCR-βδ$^{-/-}$ recipients and donor cell accumulation in recipient peripheral blood assessed by flow cytometry at the indicated weeks. Shown are CD19^{+}-gated PBL from four representative animals. Two received bPTEN/SHIP$^{-/-}$ B cells and two received WT B cells. The bPTEN/SHIP$^{-/-}$ mouse shown in the top panel died before 12 wk. (n = 8 WT recipients and 9 bPTEN/SHIP$^{-/-}$ recipients). (B) The percentage of CD5^{+}CD19^{+}B220^{low} B cells in the peripheral blood of TCR-βδ$^{-/-}$ animals after adoptive transfer of WT or bPTEN/SHIP$^{-/-}$ B cells is shown over time. Each point represents a single animal. Error bars represent SD of percentages of CD5^{+}CD19^{+}B220^{low} PBLs in chimeric mice at each time point shown. (C) Flow cytometry plots of PBLs from representative chimeras stained for CD19, B220, CD11b, CD5, and IgD. Data shown are 9 wk after transfer. (D) Kaplan-Meier survival curve of TCR-βδ$^{-/-}$ recipients after adoptive transfer of WT or bPTEN/SHIP$^{-/-}$ B cells. WT, n = 8; bPTEN/SHIP$^{-/-}$, n = 9.

of BAFF alone to induce proliferation of WT B cells results from a failure to down-regulate p27^{kip1} (Huang et al., 2004), a cyclin-dependent kinase inhibitor which is negatively regulated by Akt either directly or via inhibition of the FOXO factors. As compared with WT and single-deficient B cells, bPTEN/SHIP$^{-/-}$ B cells assayed directly ex vivo displayed diminished expression of p27^{kip1} as well as enhanced expression of cyclin D3, an indicator of entry into the G1 phase of the cell cycle (Fig. 5 B). Consistent with these results, activated Akt, indicated by phosphorylation at serine 473, was readily detected in unstimulated bPTEN/SHIP$^{-/-}$ B cells. This is in contrast to WT and single knockout controls which failed to show basal Akt activity (Fig. 5 C). These data suggest a mechanism by which bPTEN/SHIP$^{-/-}$ B cells are biochemically poised to proliferate after BAFF stimulation.

WT, bPTEN$^{-/-}$, bSHIP$^{-/-}$, and bPTEN/SHIP$^{-/-}$ B cells were stimulated in vitro with anti-IgM in the presence or absence of BAFF. Compared with controls, bPTEN/SHIP$^{-/-}$ B cells consistently showed decreased expression of p27^{kip1} and increased cyclin D3 expression under all stimulation conditions (Fig. 5 B). Furthermore, signaling through the BCR in bPTEN/SHIP$^{-/-}$ B cells in the presence or absence of BAFF also resulted in hyperactivation of Akt in bPTEN/SHIP$^{-/-}$ B cells (Fig. 5 C). Together, these data indicate that although

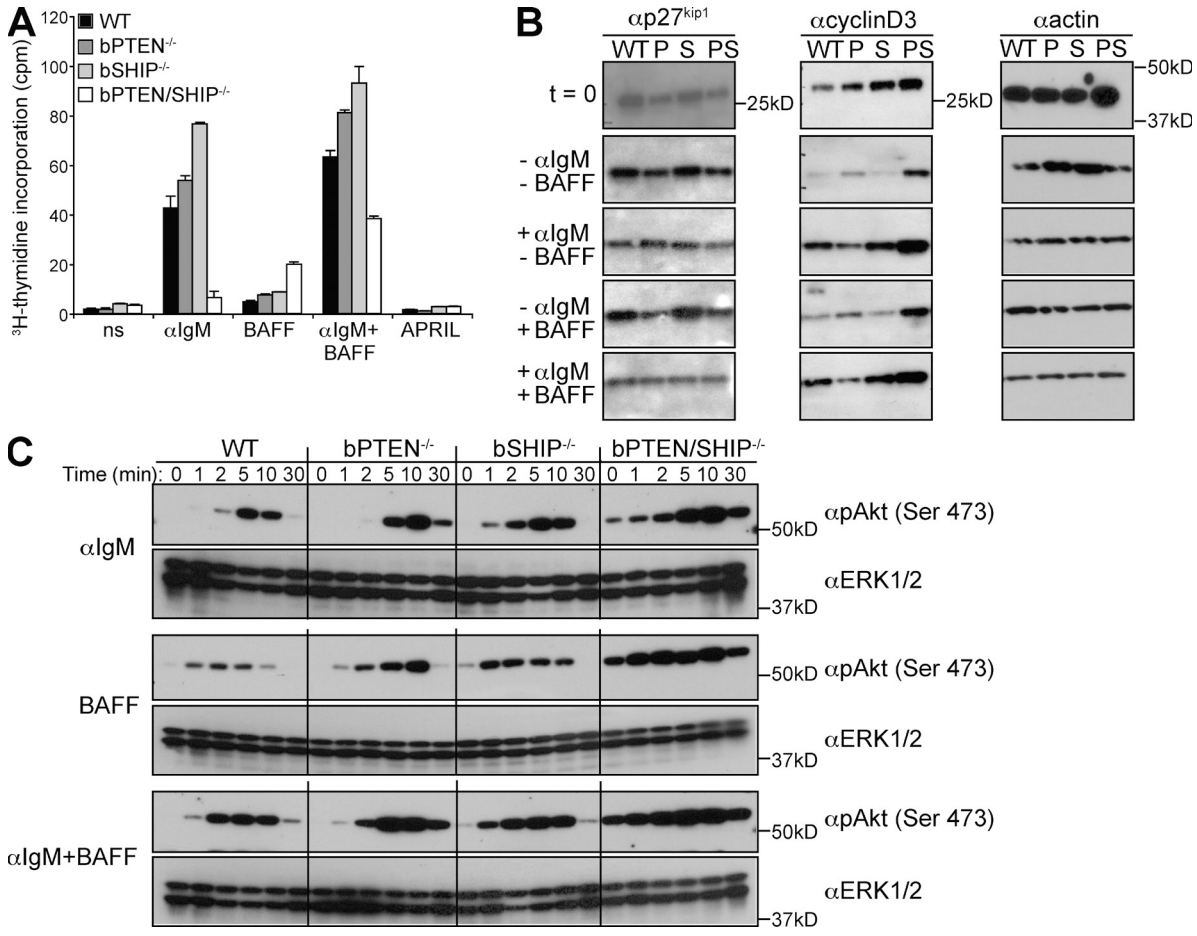

Figure 5. bPTEN/SHIP$^{-/-}$ B cells proliferate in response to treatment with BAFF. (A) Purified splenic B cells from WT, bPTEN$^{-/-}$, bSHIP$^{-/-}$, or bPTEN/SHIP$^{-/-}$ mice were stimulated with anti-IgM F(ab')$_2$ (α-IgM) in the presence or absence of BAFF or with APRIL as indicated. Proliferation was determined at 48 h by ^{3}H-thymidine incorporation. Y-axis values shown are $\times 10^{-3}$ cpm. All assays were conducted in triplicates and SDs are shown as error bars. The results are representative of six experiments. (B) Western blots of protein lysates from WT, bPTEN$^{-/-}$ (P), bSHIP$^{-/-}$ (S), or bPTEN/SHIP$^{-/-}$ (PS) splenic B cells either freshly isolated (t = 0) or stimulated for 48 h, as indicated, were probed with anti-p27^{kip1}, anti-cyclin D3, or anti-actin antibodies. (C) WT, bPTEN$^{-/-}$, bSHIP$^{-/-}$, or bPTEN/SHIP$^{-/-}$ B cells were stimulated with anti-IgM F(ab')$_2$ (α-IgM), BAFF, or anti-IgM F(ab')$_2$ (α-IgM) + BAFF for the indicated time points. Western blots were probed with antibodies recognizing the phosphorylated form of Akt (Ser 473). Total ERK1/2 was used as a loading control. For B and C, data are representative of $n = 5$ independent experiments.

bPTEN/SHIP$^{-/-}$ B cells are biochemically hyperresponsive to signals through the BCR and BAFF receptors and up-regulate cyclin D3 in response to BCR stimulation, signals through the BCR and BAFF receptors alone are likely not sufficient to support their survival and expansion in vivo.

To directly assess the contribution of BAFF signaling to lymphoma progression, WT or bPTEN/SHIP$^{-/-}$ B cells were transferred into sublethally irradiated *BAFF*$^{-/-}$ animals and monitored over a 6-mo period for the appearance of lymphoma cells in the peripheral blood. As expected, WT B cells failed to survive and expand in the absence of BAFF in vivo (Fig. S4 A). However, we found that bPTEN/SHIP$^{-/-}$ B cells were able to expand in some (4/11) *BAFF*$^{-/-}$ recipients (Fig. S4 A). This result cannot be explained by autocrine production of BAFF, as *BAFF* message was not detectable by RT-PCR analysis of bPTEN/SHIP$^{-/-}$ B cells (Fig. S4 B). Moreover, blockade of BAFF in in vitro cultures of bPTEN/SHIP$^{-/-}$ B cells did not result in reduced viability of bPTEN/SHIP$^{-/-}$ B cells as compared with untreated cells (Fig. S4 D). Thus, although BAFF provides a mitogenic signal to bPTEN/SHIP$^{-/-}$ B cells, it is not an absolute requirement for lymphoma progression in situations in which PI3K signaling is deregulated.

bPTEN/SHIP$^{-/-}$ B cells show enhanced survival

Mouse B cell lymphoma cells not only survive and expand after transfer into immunocompromised recipient animals but they also persist in vitro. Given the presence of activated Akt in freshly isolated bPTEN/SHIP$^{-/-}$ B cells (Fig. 5 C), we proceeded to examine the survival of B cells lacking expression of PTEN and/or SHIP. Splenic B cells were purified from WT, bPTEN$^{-/-}$, bSHIP$^{-/-}$, and bPTEN/SHIP$^{-/-}$ mice and cultured in the absence of mitogenic stimuli or survival factors. In contrast to their rapid in vivo expansion after transfer into TCR-βδ$^{-/-}$ hosts, bPTEN/SHIP$^{-/-}$ lymphoma cells persisted

but did not proliferate when cultured in the absence of stimulation ex vivo (Fig. 6 A). In contrast, B cells from WT and single mutant bPTEN$^{-/-}$ and bSHIP$^{-/-}$ mice did not persist and died more rapidly than bPTEN/SHIP$^{-/-}$ B cells (Fig. 6 A). In this regard, bPTEN/SHIP$^{-/-}$ B cell cultures contained an increased percentage of live cells as indicated by annexin V and propidium iodide staining compared with cultures of WT or single knockout B cells (Fig. 6 B). Consistent with increased survival and basally activated Akt (Fig. 6 C), levels of GSK3β(S9) phosphorylation, corresponding to the negative regulatory site for Akt, were also augmented in bPTEN/SHIP$^{-/-}$ B cells (Fig. 6 C). Notably, phosphorylation of Akt and GSK3β in bPTEN/SHIP$^{-/-}$ B cells was detected not only in freshly isolated B cells but also in cells from long-term culture. Consistent with inhibition of GSKβ by Akt and GSK3β-dependent degradation of the prosurvival factor MCL1 (Maurer et al., 2006), bPTEN/SHIP$^{-/-}$ B cells expressed elevated amounts of MCL1 compared with WT, bPTEN$^{-/-}$, or bSHIP$^{-/-}$ B cells at all time points examined (Fig. 6 C). Moreover, freshly isolated bPTEN/SHIP$^{-/-}$ B cells expressed lower levels of the pro-apoptotic factor and FOXO-regulated gene product Bim (Dijkers et al., 2000) than WT or bSHIP$^{-/-}$ controls (Fig. 6 D). Interestingly, bPTEN$^{-/-}$ B cells also expressed lower levels of Bim than WT or bSHIP$^{-/-}$ B cells but did not survive in vitro, suggesting that factors in addition to Bim may be responsible for the enhanced survival and expansion of bPTEN/SHIP$^{-/-}$ B cells both in vivo and in vitro.

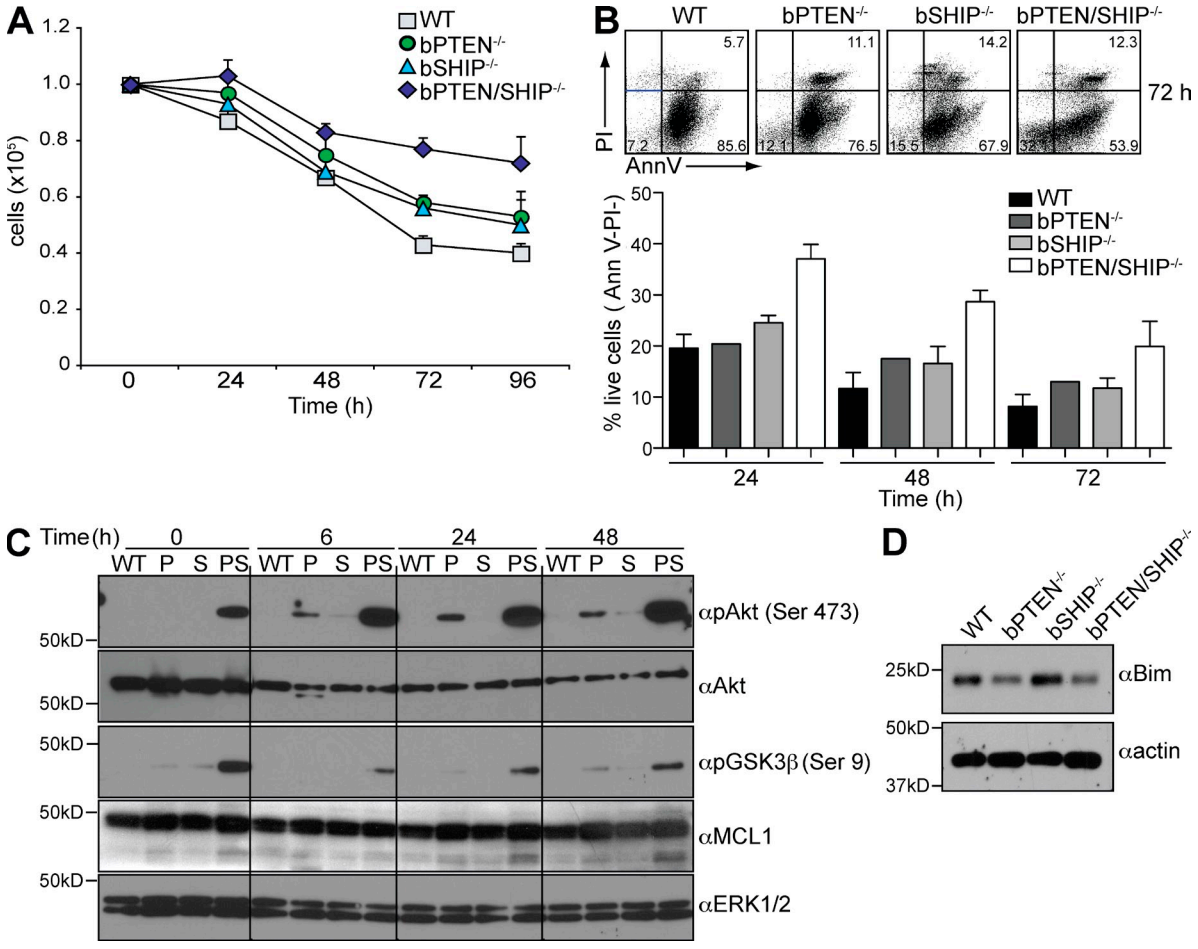

Figure 6. bPTEN/SHIP$^{-/-}$ B cells survive better than WT, bPTEN$^{-/-}$, or bSHIP$^{-/-}$ B cells in vitro. (A) WT, bPTEN$^{-/-}$, bSHIP$^{-/-}$, or bPTEN/SHIP$^{-/-}$ B cells were cultured at a starting concentration of 5 × 10^5 cells/ml in media lacking any growth factors and surviving cells were counted every 24 h using a Coulter counter. Data are representative of $n = 3$ independent experiments. Error bars represent SD of total live cells of triplicate wells counted in triplicate for each mouse. (B) As in A, with the modification that cell viability was assessed by annexin V (Ann V) and propidium iodide (PI) staining. (Top) Shown is a representative panel of WT, bPTEN$^{-/-}$, bSHIP$^{-/-}$, and bPTEN/SHIP$^{-/-}$ at 72 h (top) and a graph showing the percentage of live (Ann V-PI$^-$) cells over time (bottom). Data are representative of $n = 3$ independent experiments. Error bars represent SD of the percentage of annexin V–propidium iodide (Ann V-PI$^-$) B cells for WT, bPTEN$^{-/-}$, bSHIP$^{-/-}$, and bPTEN/SHIP$^{-/-}$ mice at each time point shown. (C) As in A, with the modification that cells were lysed at indicated time points and Western blotting performed to detect levels of pAkt (Ser 473), total Akt, pGSK3β (Ser 9), and MCL-1. Total ERK1/2 levels were used as a loading control. Data are representative of $n = 3$ independent experiments. (D) Bim expression in freshly isolated splenic WT, bPTEN$^{-/-}$, bSHIP$^{-/-}$, or bPTEN/SHIP$^{-/-}$ B cells was determined by immunoblotting with anti-Bim. Blots were stripped and reprobed with anti-actin antibodies as a loading control. Data are representative of $n = 3$ experiments.

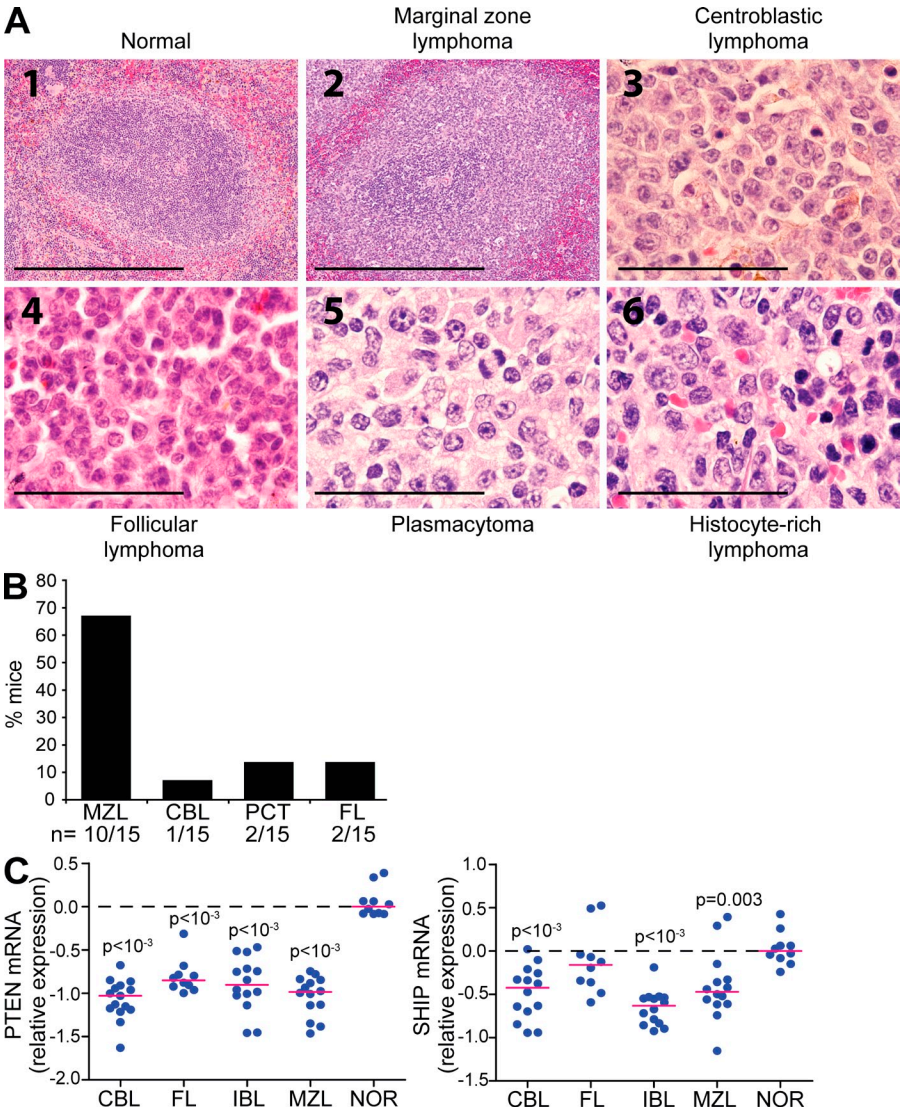

Figure 7. bPTEN/SHIP$^{-/-}$ mice develop different B cell neoplasias. (A) Representative examples of B-NHL developed by bPTEN/SHIP$^{-/-}$ mice. (1) Normal spleen (10×): white pulp follicle filled with small lymphocytes surrounded by an MZ and red pulp. (2) MZL (10×): white pulp with a periarteriolar lymphoid sheath of small lymphocytes surrounded by an expanse of uniform medium-sized MZ B cells extending into the red pulp. (3) Centroblastic lymphoma (100×): white pulp is taken over by large blasts with dispersed chromatin and one or more nucleoli, often located near the nuclear membrane. One mitotic figure is seen near the center, and multiple apoptotic bodies are present. (4) Follicular lymphoma (100×): the white pulp is occupied by a heterogeneous population of smaller centrocytes with angulated and folded nuclei as well as larger centroblasts with more dispersed chromatin and peripheral nucleoli. (5) Plasmacytoma (100×): lymph node populated with plasmablasts with thick nuclear membranes and prominent nucleoli. Plasmacytic cells with relatively condensed chromatin and central nucleoli, and a prominent mitotic figure are also present. (6) Histiocyte-associated DLBCL (100×): histiocytes with very large nuclei with reticular chromatin and irregular nucleoli are present along with an abundance of foamy pink cytoplasm. One mitotic figure can be seen in the top right. The lymphoid population is comprised of centroblasts and several immunoblasts. Bars: (1 and 2) 500 µm; (3–6) 50 µm. (B) Classification of B-NHL displayed by bPTEN/SHIP$^{-/-}$ mice as determined by histological examination of splenic samples. CBL, centroblastic lymphoma; PCT, plasmacytoma; FL, follicular lymphoma. The chart represents 15 different animals per group. (C) Relative levels of *PTEN* and *SHIP* mRNA transcripts in mouse B cell lymphoma determined by oligo-microarray. Values from 10–15 mice in each lymphoma group were tested against normal spleen by Mann-Whitney *U* test. The pink line shows the median in each group. CBL, centroblastic lymphoma; IBL, immunoblastic lymphoma; NOR, normal spleen. The mean Log_2 normalized expression of *PTEN* and *SHIP* is plotted. P-values are indicated.

Expression of PTEN and SHIP is reduced in human DLBCL

The histological and cytological features of lymphoid tissues of bPTEN/SHIP$^{-/-}$ mice were consistent with the diagnosis of B cell lymphoma. To investigate the type of lymphomas that develop in bPTEN/SHIP$^{-/-}$ animals, lymphomas were classified in accordance with the Bethesda proposals for mouse lymphoid neoplasms (Morse et al., 2002). Although the tumors of nearly all mice exhibited histological and cytological features most closely resembling those described for mouse splenic MZ lymphomas (MZL; Fig. 7, A and B; Morse et al., 2002), certain distinguishing characteristics suggested that bPTEN/SHIP$^{-/-}$ lymphomas were distinct from previously observed cases of MZL (Fredrickson et al., 1999; Morse et al., 2002; Shin et al., 2004). For example, MZLs are initially low-grade tumors restricted to the splenic MZ, which is located just outside the follicles, but later invade both the white and red pulp when they progress to high-grade tumors (Morse et al., 2002; Shin et al., 2004). Histological examination of spleen sections revealed that bPTEN/SHIP$^{-/-}$ lymphomas were localized to follicles in this organ, often completely replacing normal structures, leaving virtually no small lymphocytes in the periarteriolar lymphoid sheaths (Fig. 1 D and Fig. 7 A). Moreover, splenic red pulp involvement was less prominent compared with reported cases of MZL but exhibited similar degrees of white pulp compression (Fig. 1 D; Morse et al., 2002; Shin et al., 2004).

Low-grade MZLs are typically comprised of uniform cells of medium size that are larger than, but cytologically very similar to, normal MZ B cells (Fredrickson et al., 1999; Morse et al., 2002). In contrast, high-grade MZLs reportedly retain

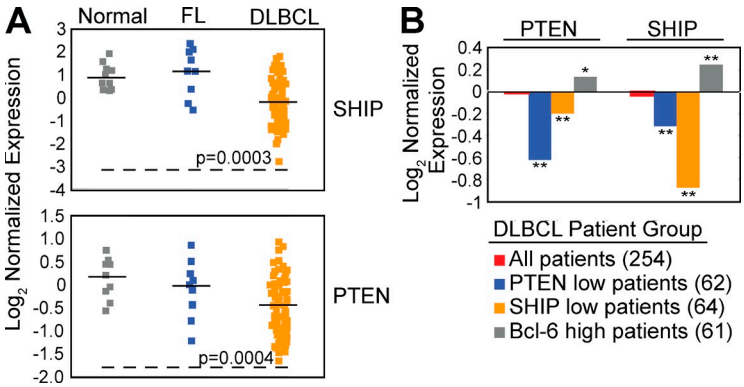

Figure 8. Human DLBCL patients exhibit reduced *PTEN* and *SHIP* expression compared with FL patients. (A) cDNA expression analysis of human malignant B cell lymphoma samples from publicly available patient data (www.oncomine.org) comparing normal B cells, FL, and DLBCL showing mean (black lines) relative expression values for *PTEN* and *SHIP* cDNA. Each square represents an expression value for a single patient/sample. P-values comparing normal cells and DLBCL cells are indicated. (B) Mean Log_2 normalized expression of *PTEN* and *SHIP* is plotted for the following patient groups: *PTEN* low (lowest 25% *PTEN* expression), *SHIP* low (lowest 25% *SHIP* expression), and *BCL6* high (highest 25% *BCL6* expression), in comparison with mean values for all patients which were near 0. Analyses of other genes in the *PTEN* and *SHIP* low patient cohort confirmed that results were not a result of generally low cDNA signals in this cohort. *, $P < 0.05$; **, $P < 0.005$.

their physical relationship to the MZ but take on features indistinguishable from those of centroblastic DLBCLs (CBLs; Fig. 7 A). Some cases of bPTEN/SHIP$^{-/-}$ lymphomas exhibited mixed cell populations of centrocytes and centroblasts, which is consistent with a diagnosis of follicular B cell lymphoma (FL), whereas others were dominated by centroblasts as seen in CBL. Still others were characterized by sheets of plasma cells, which is consistent with a diagnosis of plasmacytoma (Fig. 7, A and B). It is noteworthy that both low- and high-grade MZLs are almost always restricted to the spleen, whereas we consistently observed bPTEN/SHIP$^{-/-}$ lymphoma infiltrates in nonlymphoid tissues, including liver, lung, heart, and, occasionally, kidney (Fredrickson et al., 1999; Morse et al., 2002). bPTEN/SHIP$^{-/-}$ B cells did not predominate in the bone marrow, which occurs in B cell leukemia.

To corroborate these findings, we assessed expression of *SHIP* and *PTEN* transcripts in splenic samples from NFS.V congenic mice that spontaneously develop a spectrum of B lymphomas (Hartley et al., 2000; Shin et al., 2008). *PTEN* is down-regulated in all lymphoma types, and *SHIP* is down-regulated in two types of DLBCL (CBL and IBL) and MZL but is statistically unchanged for FL. Collectively, these findings indicate that bPTEN/SHIP$^{-/-}$ mice develop lymphomas with overlapping similarities to several previously described subsets of mouse mature B cell lymphomas.

To examine the potential utility of the bPTEN/SHIP$^{-/-}$ mouse as a model for human disease, levels of *PTEN* and/or *SHIP* transcripts in human B cell lymphomas were examined. The two most prevalent human B cell lymphomas, FL and DLBCL, represent >55% of all human mature B cell lymphomas (Evans and Hancock, 2003). Mutations that augment PI3K signaling and inactivating PTEN mutations have recently been reported in some human DLBCL cases (Uddin et al., 2006; Abubaker et al., 2007; Lenz et al., 2008). Accordingly, existing patient microarray gene expression profiling data revealed a reduction in mean *PTEN* and *SHIP* expression in DLBCL compared with normal B cells (including naive, memory, and GC B cells) and the less aggressive FL (Alizadeh et al., 2000; Fig. 8 A).

To determine if subsets of DLBCL (previously distinguished based on differences in *BCL6* expression; Alizadeh et al., 2000) could be distinguished by levels of transcripts for *PTEN* and *SHIP*, data for 254 cases of DLBCL were examined and classified into the following three groups based on *PTEN*, *SHIP*, and *BCL6* expression: (1) the 25% of cases with the lowest levels of *PTEN* transcripts; (2) the 25% of cases with the lowest levels of *SHIP* transcripts; and (3) the 25% of cases with the highest levels of *BCL6* transcripts. These analyses revealed that patient samples with the lowest relative levels of *PTEN* (group 1) had *SHIP* transcripts significantly lower than the mean for all patients (Fig. 8 B, right, blue bar). Similarly, patient samples with low *SHIP* expression (group 2) had significantly lower levels of *PTEN* transcripts than the mean for all patients (Fig. 8 B, left, orange bar). Patients with the highest levels of *BCL6* transcripts (group 3), most of which reportedly belong to the GC subset of DLBCL (Alizadeh et al., 2000), had levels of transcripts for both *PTEN* and *SHIP* that were significantly above the mean (Fig. 8 A), suggesting that the lymphomas of bPTEN/SHIP$^{-/-}$ mice are probably not closely aligned to human GC-DLBCL. These results are consistent with coordinate tumor suppressor functions of these two phosphatases in B cells.

DISCUSSION

Cellular transformation in mammals is a complex and often multigenic process. Therefore, identifying and testing the genetic and epigenetic bases of particular malignancies has been challenging. In recent years, various studies have identified the tumor suppressor PTEN as a target in multiple tumor types and disease models. Studies of malignancies driven by loss-of-function *PTEN* mutations and gain-of-function mutations in PI3K subunit genes have established the relevance of the PI3K pathway in promoting cancer (Yuan and Cantley, 2008). Surprisingly, a tumor suppressor role for *INPP5D*, the gene encoding SHIP, which also regulates PI3K signaling, has not been demonstrated (Rohrschneider et al., 2000). In this paper, we provide the first evidence that SHIP acts as a tumor suppressor and that it acts in concert with PTEN to suppress B cell transformation.

Elevated PI3K signaling has recently been noted in selected B cell malignancies, namely MCL and DLBCL (Rudelius et al., 2006; Uddin et al., 2006). MCL patients are highly responsive to rapamycin treatment to inactivate mTOR activity (Witzig

and Kaufmann, 2006), and Akt activity is enhanced in many MCL lines that are dependent on PI3K for cell cycle progression and survival (Rudelius et al., 2006). Similarly, bPTEN/SHIP$^{-/-}$ lymphoma cells are responsive to PI3K inhibitors and rapamycin (unpublished data). Although the incidence of mutations in *PTEN* in human cancers is second only to that of *TP53* (Stiles et al., 2004; Cully et al., 2006), we previously found that its loss in B cells does not cause transformation (Anzelon et al., 2003). In the case of DLBCL, reduced PTEN expression or predicted oncogenic *PIK3CA* mutations occurred in 37 and 8% of cases, respectively. Both alterations were associated with poor overall survival (Abubaker et al., 2007). Consistent with these findings, PTEN expression was reduced but still present in primary MCL cases exhibiting elevated Akt activity (Rudelius et al., 2006), raising the possibility that SHIP expression or function may also be affected.

Importantly, *SHIP* has recently been identified as a miR-155 target, causing reduced SHIP expression in a subset of DLBCL cases (Pedersen et al., 2009). This finding was confirmed in a miR-155 transgenic B lymphoma model (Costinean et al., 2009) and also reported in macrophages responding to inflammatory stimuli (O'Connell et al., 2009). Intriguingly, these findings suggest that epigenetic down-regulation of SHIP expression by inflammation-induced miR-155 expression may promote transformation of B cells with impaired PTEN function.

PTEN regulates PI(3,4,5)P_3 levels in all resting and stimulated cells. SHIP, in contrast, is expressed only in hematopoietic cells and depends on membrane recruitment via phosphotyrosine residues or SH3-based interactions for its activation (Leslie et al., 2008). In particular, upon recruitment to ITIM residues after coengagement with FcγRIIB, SHIP mediates an inhibitory effect on BCR signaling. Thus, in the absence of PTEN, BCR-induced PI(3,4,5)P_3 production likely remains dampened by SHIP. Accordingly, we postulate that disease in bPTEN/SHIP$^{-/-}$ mice is promoted, at least in part, by tonic and/or antigen-mediated BCR signaling, which becomes lymphomagenic in the absence of both phosphatases. Indeed, BCR recognition of microbial or auto-antigens is thought to promote B-NHLs including MZL, CLL, and FL (Damle et al., 1999; Guyomard et al., 2003; Hervé et al., 2005). Clonal bPTEN/SHIP$^{-/-}$ lymphoma populations support a role for antigen-mediated selection in lymphomagenesis. Moreover, heightened serum IgM and IgM deposits in bPTEN/SHIP$^{-/-}$ heart and kidneys (unpublished data) are consistent with poly- or autoreactive antigen receptor signaling that may help drive lymphoma expansion in this animal model. Interestingly, however, bPTEN/SHIP$^{-/-}$ lymphoma cells, which do not spontaneously proliferate, are also quite hypoproliferative in response to BCR stimulation in ex vivo cultures. It is possible that this reflects a refractory or tolerized state, perhaps caused by sustained antigen receptor ligation or tonic signaling. However, biochemistry studies indicate that Akt and other downstream effectors of the PI3K pathway are hyperactivated both basally and after various stimuli, including ligation of the antigen receptor. Thus, it is clear that B cells lacking PTEN and SHIP are not completely refractory to BCR ligation and that activation of PI3K effectors are enhanced after this stimulus. This observation, taken with the collective results presented here, suggests that despite the hypoproliferative phenotype observed ex vivo, bPTEN/SHIP$^{-/-}$ lymphoma progression is driven, at least partly, by signals through the antigen receptor but likely requires the contribution of additional receptor-mediated signals.

In this regard, BAFF, which promotes B cell survival and supports BCR-dependent clonal expansion of normal B cells, is an attractive candidate. BAFF activates B cells to enter G_1 phase of the cell cycle marked by up-regulation of cyclin D, but cell cycle progression is halted before S phase without p27 down-regulation and cyclin E up-regulation (Huang et al., 2004). Notably, here we found that BAFF alone stimulated proliferation of bPTEN/SHIP$^{-/-}$ B cells and that the combination of BAFF and anti-IgM stimuli synergistically enhanced proliferation. Indeed, in addition to its role in dampening BCR signaling, SHIP has been linked to suppression of BAFF-induced signals and acts in a BCR-dependent fashion to suppress signaling via other receptors such as CXCR4 (Brauweiler et al., 2007; Crowley et al., 2009). Thus, it is possible that in the absence of PTEN, SHIP prevents transformation by regulating PIP_3 levels induced by the BCR and other mitogenic signals and that in the absence of both phosphatases, the combination of unchecked signals via multiple receptors promotes disease.

A role for BAFF in B cell malignancies has been suggested. Transgenic expression of either BAFF (when combined with TNF deficiency) or the related molecule APRIL results in B cell neoplasia in mice (Mackay et al., 1999; Planelles et al., 2004). Studies in humans implicate BAFF and/or APRIL in mature B cell lymphomas, multiple myeloma, B cell chronic lymphocytic leukemia, and Waldenstrom's macroglobulinemia (Shivakumar and Ansell, 2006; Tangye et al., 2006). We did not find evidence of autocrine BAFF production by bPTEN/SHIP$^{-/-}$ cells. Moreover, serum BAFF levels were not reduced, even in mice bearing a large tumor load (unpublished data), confirming that BAFF is not limiting in vivo. bPTEN/SHIP$^{-/-}$ B cells acquire the ability to proliferate to BAFF, which typically only promotes survival. Although BAFF is absolutely required for late maturation of WT B cells, transfer of bPTEN/SHIP$^{-/-}$ B cells into *BAFF*$^{-/-}$ recipients showed that its presence is not a strict requirement for B lymphoma progression. Nonetheless, lymphoma progression appeared to be less aggressive in BAFF$^{-/-}$ than in TCR-β/δ$^{-/-}$ recipients, suggesting that acute depletion of BAFF could deliver a therapeutic benefit in reducing tumor burden.

In summary, the bPTEN/SHIP$^{-/-}$ model presented in this paper provides the first evidence that SHIP is a tumor suppressor. As such, this model will be useful for elucidating the specific roles of PTEN and SHIP in B cell neoplasia, as well as providing a novel platform for interrogating and therapeutically manipulating the PI3K pathway in cancer. In a broader sense, the bPTEN/SHIP$^{-/-}$ mice also provide a system with which to investigate B cell–intrinsic (e.g., the BCR) and microenvironmental (e.g., BAFF/APRIL) factors that promote lymphoma induction and progression.

MATERIALS AND METHODS

Generation of bPTEN$^{-/-}$, bSHIP$^{-/-}$, and bPTEN/SHIP$^{-/-}$ mice. bPTEN$^{-/-}$ mice were generated as previously described (Anzelon et al., 2003). bSHIP$^{-/-}$ mice were generated by crossing SHIP$^{flox/flox}$ (Karlsson et al., 2003) mice with *Cd19Cre* mice (Rickert et al., 1997) to generate B cell–specific deletion of SHIP. bPTEN/SHIP$^{-/-}$ mice were generated by crossing PTEN$^{flox/flox}$ (Lesche et al., 2002), SHIP$^{flox/flox}$, and *Cd19Cre*$^{+/-}$ mice. All animals were heterozygous for *Cd19Cre* to achieve deletion of loxP-flanked exons while maintaining one CD19 allele. TCR-βδ$^{-/-}$ mice were purchased from The Jackson Laboratory. All animals were maintained in the animal facility of the Sanford-Burnham Medical Research Institute (SBMRI). All protocols were approved by the Institutional Animal Care and Use Committee at the SBMRI and were performed in accordance with institutional guidelines and regulations.

Mouse viability and disease analysis. To assess disease progression and animal viability/morbidity, cohorts of 15–20 animals per genotype were monitored over the course of 1 yr. Animals displaying signs of morbidity (lethargy, severe weight loss, hunched posture, ruffled fur, and slow movement) were considered morbid, euthanized, and scored as nonsurviving (note: if left alone, mice die within 2–3 d of development of the symptoms described). Hematology, including differentials and cytology, was performed by the University of California San Diego (UCSD) Animal Care Program Diagnostic Laboratory.

Histology. For paraffin-embedded sections, tissues were fixed immediately after harvest in 4% paraformaldehyde (Polysciences Inc.) for 24–48 h and stored in 95% ethanol. Paraffin embedding, sectioning, and H&E staining were performed by the UCSD Cancer Center and by the SBMRI Histology Core facilities according to standard protocols. Immunofluorescent staining of frozen tissue sections was performed as previously described (Anzelon et al., 2003) with indicated antibodies and reagents (see Flow cytometry and antibodies).

Flow cytometry and antibodies. Single cell suspensions were prepared, counted, and stained with antibodies according to standard procedures. First, cells were stained for 20 min at 4°C with biotinylated antibodies in flow cytometry buffer (1% FBS and 0.1% azide in PBS), followed by incubation with a cocktail of antibodies conjugated to FITC, PE, peridinin chlorophyll protein complex–cyanine 5.5 (PerCP-Cy5.5.), PE-indotricarbocyanine (PE-Cy7), allophycocyanin (APC), or APC-Cy7. The following antibody conjugates were used (eBioscience): CD3 (145-2C11), IgM (II/41), IgD (11–26), CD5 (53–7.3), CD19 (ID3), B220 (RA3-6B2), CD11b (M1/70), CD43 (S7), CD21 (4E3), CD23 (B3B4), F4/80 (BM8), Gr1 (RB6-8C5), CD4 (GK1.5), CD8 (53–6.7), and CD11c (N418). Biotinylated reagents were detected with streptavidin (SAV) conjugated to FITC, PE, APC, PerCP-Cy5.5 (BD), and PE-Cy7 (eBioscience). All data were collected on a FACSCanto flow cytometer (BD) and analyzed using FlowJo software (Tree Star, Inc.). Data are displayed with logarithmic scale. Each plot represents analysis of 1–3 × 10^4 events.

Assessment of IgH rearrangements. B cells were purified from spleen cell suspensions by magnetic removal of cells stained with biotinylated antibodies against CD4 (GK1.5), CD3 (145-2C11), CD11c (N418), and Gr-1 (RB6-8C5; eBioscience) followed by negative selection with anti-biotin–conjugated MACS beads (Miltenyi Biotec). Purity of B cells routinely exceeded 85% as determined by flow cytometry. For Southern blot analysis, genomic DNA was digested with EcoRI, fractionated on a 1% agarose gel, and transferred to Zeta probe membrane (Bio-Rad Laboratories) followed by hybridization with oligonucleotide *pJ11* probe. The probe was labeled by random hexamer priming using α-[^{32}P]dCTP.

For PCR analysis, DNA was isolated using phenol-chloroform extraction and was subjected to PCR using one of two degenerate 5′ primers homologous to sequences from one of two different V_H families (J558, 5′-CGAGCTCTCCARCACAGCCTWCATGCATCTCARC-3′; and 7183, 5′-CGGTACCAAGAASAMCCTGTWCCTGCAAATGASC-3′) and a common 3′ J_H4 primer (5′-TCCCTCAAATGAGCCTCCAAAGTCC-3′). Degenerate nucleotide positions are coded as: R = A or G; W = A or T; S = C or G; and M = A or C. PCR products generated represent *V-DJ*$_H$ rearrangements having V_H segments from either the distal *J558* (*VH1*) family or the proximal *7183* (*VH5*) family. Separation on a 1.5% agarose gel allowed for size-based separation of *V-DJ*$_H$ products containing J_H1 (1.3 kb), J_H2 (0.95 kb), and J_H3 (0.4 kb) segments.

Adoptive transfers. B cells were purified from spleen cell as described in Assessment of IgH rearrangements. For transfers into TCR-βδ$^{-/-}$ recipients, 10^7 WT or bPTEN/SHIP$^{-/-}$ B cells were injected into unmanipulated recipient animals via the tail vein. For transfers into BAFF$^{-/-}$ recipients, BAFF$^{-/-}$ mice were sublethally irradiated (5 Gy), followed by injection of 10^7 WT or bPTEN/SHIP$^{-/-}$ B cells via the tail vein. Presence of WT and bPTEN/SHIP$^{-/-}$ was monitored by reduced expression of CD19 (as a result of CD19 heterozygosity) and later by lymphoma-like phenotype (B220$^{-/low}$ CD5$^+$CD11b$^+$CD43$^+$IgM^{lo}) of bPTEN/SHIP$^{-/-}$ B cells.

Cell culture, survival, and proliferation assays. B cells were purified from spleen cell suspensions according to standard procedures and cultured in DME medium supplemented with 10% FCS, pen/strep, L-glutamine, Na-pyruvate, nonessential amino acids, and 2-mercaptoethanol (10% media). For proliferation assays, purified B cells were cultured at a concentration of 5 × 10^4 cells/100 μl in 96-well round-bottom tissue culture plates at 37°C with 10 μg/ml anti-IgM F(ab')$_2$ fragments (Jackson ImmunoResearch Laboratories) in the presence or absence of 25 ng/ml BAFF (R&D Systems) or 100 ng/ml APRIL (PeproTech), as indicated. Cells were pulsed with 1 μCi ^{3}H-thymidine at 48 h for an additional 12–16 h and then collected and scintillation counted. The data are displayed as raw cpm values. All assays were conducted in triplicate. For survival assays, 200 μl of purified splenic B cells was plated in flat-bottom 96-well plates in triplicate at a concentration of 5 × 10^5 cells/ml in 10% media. For assays involving BAFF blockade, cells were either cultured in media alone or in the presence of 10 ng/ml BAFF. Anti-BAFF IgG and control IgG (R&D Systems) were used at a concentration of 500 ng/ml. Every 24 h, cells were harvested and counted in triplicate using a Coulter counter (Beckman Coulter). Data are presented as averaged total cell numbers of three wells counted three times. Survival was also determined by flow cytometry using the AnnV-FITC Apoptosis Detection kit (BioVision Inc.) according to manufacturer's instructions.

Immunoblotting. Purified B cells were stimulated with 10 μg/ml anti-IgM F(ab')$_2$ fragments in the presence or absence of 25 ng/ml BAFF for the indicated time points and lysed on ice with RIPA buffer (PBS, 1% NP-40, 0.5% deoxycholate, 0.1% SDS, and 10 mM EDTA) supplemented with a protease inhibitor cocktail (Boehringer Mannheim), 10 mM NaF, 1 mM Na_3VO_4, and PMSF. Protein content of cleared lysates was measured using the BCA Protein Assay kit (Thermo Fisher Scientific), and equal protein amounts were resolved on 10% Bis-Tris Gels (Bio-Rad Laboratories or Invitrogen) followed by Western blotting for the indicated proteins. Antibodies raised against p27^{kip1}, cyclin D3, actin, phospho-Akt (S473), total Akt, phospho-GSK3β (S9), total ERK1/2, and Bim were obtained from Cell Signaling Technology. Anti-MCL1 was purchased from Rockland Immunochemicals. Total anti-GSK3β was purchased from Millipore. Primary antibodies were detected using horseradish peroxidase–labeled donkey anti–rabbit (Jackson ImmunoResearch Laboratories) or anti–mouse antibodies (GE Healthcare). Immune complexes were detected by SuperSignal West Pico Detection chemiluminescence (Thermo Fisher Scientific).

cDNA microarray and analysis. Relative *SHIP* and *PTEN* transcript abundance in human samples was acquired from data provided by Alizadeh et al. (2000) via the Oncomine Cancer Profiling Database (www.oncomine.org). To obtain reported values, Alizadeh et al. (2000) normalized all raw array signals to the median chip expression signal (median expression = 1), followed by Log_2 transformation (Log_2 values of 0 indicate mean expression across entire genome). For analysis of *PTEN/SHIP* co–down-regulation in human diseases, relative phosphatase expression among DLBCL patient subsets was determined using microarray data for 254 patients from Rosenwald et al. (2002; available at http://llmpp.nih.gov/DLBCL/). Mean expression values of *PTEN* (probe U92436), *SHIP* (probe U57650), and *BCL6* (probe U00115)

were calculated in patient subgroups. Low and high expression groups were defined as the lowest or highest 25% for gene expression among all patients. P-values were calculated using a two-tailed unpaired Student's *t* test assuming equal variance.

The relative transcript levels of *SHIP* and *PTEN* in mouse B cell lymphoma were determined by oligonucleotide arrays (available at GEO Datasets under accession no. GSE12157). The origins and characteristics of primary mouse B cell lineage lymphomas from NFS.V^+ congenic and the techniques used for transcriptional profiling of those lymphomas were detailed previously (Lee et al., 2006; Shin et al., 2008).

Online supplemental material. Fig. S1 shows that PTEN and SHIP are efficiently deleted in splenic bPTEN/$SHIP^{-/-}$ B cells. Fig. S2 shows that bPTEN/$SHIP^{-/-}$ B cells have clonal Ig repertoires before and after adoptive transfer into TCR-$\beta\delta^{-/-}$ recipients in contrast with WT B cells which are polyclonal. Fig. S3 shows poor proliferation of bPTEN/$SHIP^{-/-}$ B cells in response to anti-IgM stimulation but robust proliferation of bPTEN/$SHIP^{-/-}$ B cells after LPS or anti-CD40 stimulation. Fig. S4 shows that bPTEN/$SHIP^{-/-}$ B cells can survive and expand after adoptive transfer into $BAFF^{-/-}$ recipients but do not produce autocrine BAFF. Online supplemental material is available at http://www.jem.org/cgi/content/full/jem.20091962/DC1.

We thank Dr. Lou Staudt and colleagues for making publicly available the mRNA array data and prognostic information from their analyses of DLBCL patients; Nissi Varki at the University of California, San Diego Cancer Center Histology Core and Robin Newlin at the Sanford-Burnham Medical Research Institute (SBMRI) Histology Core for tissue processing, staining, and analysis; M. Scott (Biogen) for the $BAFF^{-/-}$ animals; the SBMRI animal care staff; Dr. M. David; and members of the Rickert laboratory for discussions and critical evaluation of the manuscript.

This work was supported by National Institutes of Health Grants HL088686 and CA135531 (R.C. Rickert), F32CA132350 (A.V. Miletic), and K01CA122192 (I.M. Pedersen). D.M. Mills was supported by an Arthritis Foundation Postdoctoral Fellowship. A.V. Miletic was supported by an Irvington Institute for the Cancer Research Institute Postdoctoral Fellowship. This work was also supported, in part, by the Intramural Research Program of the National Institutes of Health, National Institute of Allergy and Infectious Diseases (H.C. Morse, D-M. Shin, and S. Bolland).

The authors have no conflicting financial interests.

Submitted: 9 September 2009
Accepted: 16 September 2010

REFERENCES

Abubaker, J., P.P. Bavi, S. Al-Harbi, A.K. Siraj, F. Al-Dayel, S. Uddin, and K. Al-Kuraya. 2007. PIK3CA mutations are mutually exclusive with PTEN loss in diffuse large B-cell lymphoma. *Leukemia*. 21:2368–2370. doi:10.1038/sj.leu.2404873

Alizadeh, A.A., M.B. Eisen, R.E. Davis, C. Ma, I.S. Lossos, A. Rosenwald, J.C. Boldrick, H. Sabet, T. Tran, X. Yu, et al. 2000. Distinct types of diffuse large B-cell lymphoma identified by gene expression profiling. *Nature*. 403:503–511. doi:10.1038/35000501

Anzelon, A.N., H. Wu, and R.C. Rickert. 2003. Pten inactivation alters peripheral B lymphocyte fate and reconstitutes CD19 function. *Nat. Immunol.* 4:287–294. doi:10.1038/ni892

Barragán, M., B. Bellosillo, C. Campàs, D. Colomer, G. Pons, and J. Gil. 2002. Involvement of protein kinase C and phosphatidylinositol 3-kinase pathways in the survival of B-cell chronic lymphocytic leukemia cells. *Blood*. 99:2969–2976. doi:10.1182/blood.V99.8.2969

Brauweiler, A., I. Tamir, J. Dal Porto, R.J. Benschop, C.D. Helgason, R.K. Humphries, J.H. Freed, and J.C. Cambier. 2000a. Differential regulation of B cell development, activation, and death by the src homology 2 domain-containing 5′ inositol phosphatase (SHIP). *J. Exp. Med.* 191:1545–1554. doi:10.1084/jem.191.9.1545

Brauweiler, A.M., I. Tamir, and J.C. Cambier. 2000b. Bilevel control of B-cell activation by the inositol 5-phosphatase SHIP. *Immunol. Rev.* 176:69–74. doi:10.1034/j.1600-065X.2000.00612.x

Brauweiler, A., K. Merrell, S.B. Gauld, and J.C. Cambier. 2007. Cutting Edge: Acute and chronic exposure of immature B cells to antigen leads to impaired homing and SHIP1-dependent reduction in stromal cell-derived factor-1 responsiveness. *J. Immunol.* 178:3353–3357.

Butler, M.P., S.I. Wang, R.S. Chaganti, R. Parsons, and R. Dalla-Favera. 1999. Analysis of PTEN mutations and deletions in B-cell non-Hodgkin's lymphomas. *Genes Chromosomes Cancer*. 24:322–327. doi:10.1002/(SICI)1098-2264(199904)24:4<322::AID-GCC5>3.0.CO;2-9

Costinean, S., S.K. Sandhu, I.M. Pedersen, E. Tili, R. Trotta, D. Perrotti, D. Ciarlariello, P. Neviani, J. Harb, L.R. Kauffman, et al. 2009. Src homology 2 domain–containing inositol-5-phosphatase and CCAAT enhancer-binding protein β are targeted by miR-155 in B cells of Eμ-*MiR-155* transgenic mice. *Blood*. 114:1374–1382. doi:10.1182/blood-2009-05-220814

Crowley, J.E., J.E. Stadanlick, J.C. Cambier, and M.P. Cancro. 2009. FcgammaRIIB signals inhibit BLyS signaling and BCR-mediated BLyS receptor up-regulation. *Blood*. 113:1464–1473. doi:10.1182/blood-2008-02-138651

Cully, M., H. You, A.J. Levine, and T.W. Mak. 2006. Beyond PTEN mutations: the PI3K pathway as an integrator of multiple inputs during tumorigenesis. *Nat. Rev. Cancer*. 6:184–192. doi:10.1038/nrc1819

Cuní, S., P. Pérez-Aciego, G. Pérez-Chacón, J.A. Vargas, A. Sánchez, F.M. Martín-Saavedra, S. Ballester, J. García-Marco, J. Jordá, and A. Durántez. 2004. A sustained activation of PI3K/NF-kappaB pathway is critical for the survival of chronic lymphocytic leukemia B cells. *Leukemia*. 18:1391–1400. doi:10.1038/sj.leu.2403398

Damle, R.N., T. Wasil, F. Fais, F. Ghiotto, A. Valetto, S.L. Allen, A. Buchbinder, D. Budman, K. Dittmar, J. Kolitz, et al. 1999. Ig V gene mutation status and CD38 expression as novel prognostic indicators in chronic lymphocytic leukemia. *Blood*. 94:1840–1847.

Dijkers, P.F., R.H. Medema, J.W. Lammers, L. Koenderman, and P.J. Coffer. 2000. Expression of the pro-apoptotic Bcl-2 family member Bim is regulated by the forkhead transcription factor FKHR-L1. *Curr. Biol.* 10:1201–1204. doi:10.1016/S0960-9822(00)00728-4

Donahue, A.C., and D.A. Fruman. 2004. PI3K signaling controls cell fate at many points in B lymphocyte development and activation. *Semin. Cell Dev. Biol.* 15:183–197. doi:10.1016/j.semcdb.2003.12.024

Evans, L.S., and B.W. Hancock. 2003. Non-Hodgkin lymphoma. *Lancet*. 362:139–146. doi:10.1016/S0140-6736(03)13868-8

Fredrickson, T.N., K. Lennert, S.K. Chattopadhyay, H.C. Morse III, and J.W. Hartley. 1999. Splenic marginal zone lymphomas of mice. *Am. J. Pathol.* 154:805–812.

Guyomard, S., G. Salles, M. Coudurier, H. Rousset, B. Coiffier, J. Bienvenu, and N. Fabien. 2003. Prevalence and pattern of antinuclear autoantibodies in 347 patients with non-Hodgkin's lymphoma. *Br. J. Haematol.* 123:90–99. doi:10.1046/j.1365-2141.2003.04587.x

Hardy, R.R. 2006. B-1 B cell development. *J. Immunol.* 177:2749–2754.

Hartley, J.W., S.K. Chattopadhyay, M.R. Lander, L. Taddesse-Heath, Z. Naghashfar, H.C. Morse III, and T.N. Fredrickson. 2000. Accelerated appearance of multiple B cell lymphoma types in NFS/N mice congenic for ecotropic murine leukemia viruses. *Lab. Invest.* 80:159–169. doi:10.1038/labinvest.3780020

Helgason, C.D., C.P. Kalberer, J.E. Damen, S.M. Chappel, N. Pineault, G. Krystal, and R.K. Humphries. 2000. A dual role for Src homology 2 domain-containing inositol-5-phosphatase (SHIP) in immunity: aberrant development and enhanced function of b lymphocytes in $ship^{-/-}$ mice. *J. Exp. Med.* 191:781–794. doi:10.1084/jem.191.5.781

Hervé, M., K. Xu, Y.-S. Ng, H. Wardemann, E. Albesiano, B.T. Messmer, N. Chiorazzi, and E. Meffre. 2005. Unmutated and mutated chronic lymphocytic leukemias derive from self-reactive B cell precursors despite expressing different antibody reactivity. *J. Clin. Invest.* 115:1636–1643. doi:10.1172/JCI24387

Huang, X., M. Di Liberto, A.F. Cunningham, L. Kang, S. Cheng, S. Ely, H.C. Liou, I.C. Maclennan, and S. Chen-Kiang. 2004. Homeostatic cell-cycle control by BLyS: Induction of cell-cycle entry but not G1/S transition in opposition to p18INK4c and p27Kip1. *Proc. Natl. Acad. Sci. USA*. 101:17789–17794. doi:10.1073/pnas.0406111101

Karlsson, M.C., R. Guinamard, S. Bolland, M. Sankala, R.M. Steinman, and J.V. Ravetch. 2003. Macrophages control the retention and trafficking of B lymphocytes in the splenic marginal zone. *J. Exp. Med.* 198:333–340. doi:10.1084/jem.20030684

Kraus, M., M.B. Alimzhanov, N. Rajewsky, and K. Rajewsky. 2004. Survival of resting mature B lymphocytes depends on BCR signaling via the Igalpha/beta heterodimer. *Cell*. 117:787–800. doi:10.1016/j.cell.2004.05.014

Lam, K.P., R. Kühn, and K. Rajewsky. 1997. In vivo ablation of surface immunoglobulin on mature B cells by inducible gene targeting results in rapid cell death. *Cell*. 90:1073–1083. doi:10.1016/S0092-8674(00)80373-6

Lee, C.H., M. Melchers, H. Wang, T.A. Torrey, R. Slota, C.F. Qi, J.Y. Kim, P. Lugar, H.J. Kong, L. Farrington, et al. 2006. Regulation of the germinal center gene program by interferon (IFN) regulatory factor 8/IFN consensus sequence-binding protein. *J. Exp. Med*. 203:63–72. doi:10.1084/jem.20051450

Lenz, G., G.W. Wright, N.C.T. Emre, H. Kohlhammer, S.S. Dave, R.E. Davis, S. Carty, L.T. Lam, A.L. Shaffer, W. Xiao, et al. 2008. Molecular subtypes of diffuse large B-cell lymphoma arise by distinct genetic pathways. *Proc. Natl. Acad. Sci. USA*. 105:13520–13525. doi:10.1073/pnas.0804295105

Lesche, R., M. Groszer, J. Gao, Y. Wang, A. Messing, H. Sun, X. Liu, and H. Wu. 2002. Cre/loxP-mediated inactivation of the murine Pten tumor suppressor gene. *Genesis*. 32:148–149. doi:10.1002/gene.10036

Leslie, N.R., I.H. Batty, H. Maccario, L. Davidson, and C.P. Downes. 2008. Understanding PTEN regulation: PIP2, polarity and protein stability. *Oncogene*. 27:5464–5476. doi:10.1038/onc.2008.243

Liu, Q., A.J. Oliveira-Dos-Santos, S. Mariathasan, D. Bouchard, J. Jones, R. Sarao, I. Kozieradzki, P.S. Ohashi, J.M. Penninger, and D.J. Dumont. 1998. The inositol polyphosphate 5-phosphatase ship is a crucial negative regulator of B cell antigen receptor signaling. *J. Exp. Med*. 188:1333–1342. doi:10.1084/jem.188.7.1333

Mackay, F., and P. Schneider. 2009. Cracking the BAFF code. *Nat. Rev. Immunol*. 9:491–502. doi:10.1038/nri2572

Mackay, F., S.A. Woodcock, P. Lawton, C. Ambrose, M. Baetscher, P. Schneider, J. Tschopp, and J.L. Browning. 1999. Mice transgenic for BAFF develop lymphocytic disorders along with autoimmune manifestations. *J. Exp. Med*. 190:1697–1710. doi:10.1084/jem.190.11.1697

Maurer, U., C.Charvet, A.S.Wagman, E.Dejardin, and D.R. Green. 2006. Glycogen synthase kinase-3 regulates mitochondrial outer membrane permeabilization and apoptosis by destabilization of MCL-1. *Mol. Cell*. 21:749–760.

Morse, H.C. III, M.R. Anver, T.N. Fredrickson, D.C. Haines, A.W. Harris, N.L. Harris, E.S. Jaffe, S.C. Kogan, I.C. MacLennan, P.K. Pattengale, and J.M. Ward; Hematopathology subcommittee of the Mouse Models of Human Cancers Consortium. 2002. Bethesda proposals for classification of lymphoid neoplasms in mice. *Blood*. 100:246–258. doi:10.1182/blood.V100.1.246

O'Connell, R.M., A.A. Chaudhuri, D.S. Rao, and D. Baltimore. 2009. Inositol phosphatase SHIP1 is a primary target of miR-155. *Proc. Natl. Acad. Sci. USA*. 106:7113–7118. doi:10.1073/pnas.0902636106

Pedersen, I.M., D. Otero, E. Kao, A.V. Miletic, C. Hother, E. Ralfkiaer, R.C. Rickert, K. Gronbaek, and M. David. 2009. Onco-miR-155 targets SHIP1 to promote TNFalpha-dependent growth of B cell lymphomas. *EMBO Mol Med*. 1:288–295. doi:10.1002/emmm.200900028

Planelles, L., C.E. Carvalho-Pinto, G. Hardenberg, S. Smaniotto, W. Savino, R. Gómez-Caro, M. Alvarez-Mon, J. de Jong, E. Eldering, C. Martínez-A, et al. 2004. APRIL promotes B-1 cell-associated neoplasm. *Cancer Cell*. 6:399–408. doi:10.1016/j.ccr.2004.08.033

Rickert, R.C., J. Roes, and K. Rajewsky. 1997. B lymphocyte-specific, Cre-mediated mutagenesis in mice. *Nucleic Acids Res*. 25:1317–1318. doi:10.1093/nar/25.6.1317

Rohrschneider, L.R., J.F. Fuller, I. Wolf, Y. Liu, and D.M. Lucas. 2000. Structure, function, and biology of SHIP proteins. *Genes Dev*. 14:505–520.

Rosenwald, A., G. Wright, W.C. Chan, J.M. Connors, E. Campo, R.I. Fisher, R.D. Gascoyne, H.K. Muller-Hermelink, E.B. Smeland, J.M. Giltnane, et al; Lymphoma/Leukemia Molecular Profiling Project. 2002. The use of molecular profiling to predict survival after chemotherapy for diffuse large-B-cell lymphoma. *N. Engl. J. Med*. 346:1937–1947. doi:10.1056/NEJMoa012914

Rudelius, M., S. Pittaluga, S. Nishizuka, T.H. Pham, F. Fend, E.S. Jaffe, L. Quintanilla-Martinez, and M. Raffeld. 2006. Constitutive activation of Akt contributes to the pathogenesis and survival of mantle cell lymphoma. *Blood*. 108:1668–1676. doi:10.1182/blood-2006-04-015586

Sakai, A., C. Thieblemont, A. Wellmann, E.S. Jaffe, and M. Raffeld. 1998. PTEN gene alterations in lymphoid neoplasms. *Blood*. 92:3410–3415.

Shin, M.S., T.N. Fredrickson, J.W. Hartley, T. Suzuki, K. Akagi, K. Agaki, and H.C. Morse III. 2004. High-throughput retroviral tagging for identification of genes involved in initiation and progression of mouse splenic marginal zone lymphomas. *Cancer Res*. 64:4419–4427. doi:10.1158/0008-5472.CAN-03-3885

Shin, D.M., D.J. Shaffer, H. Wang, D.C. Roopenian, and H.C. Morse III. 2008. NOTCH is part of the transcriptional network regulating cell growth and survival in mouse plasmacytomas. *Cancer Res*. 68:9202–9211. doi:10.1158/0008-5472.CAN-07-6555

Shivakumar, L., and S. Ansell. 2006. Targeting B-lymphocyte stimulator/B-cell activating factor and a proliferation-inducing ligand in hematologic malignancies. *Clin. Lymphoma Myeloma*. 7:106–108. doi:10.3816/CLM.2006.n.046

Smith, P.G., F. Wang, K.N. Wilkinson, K.J. Savage, U. Klein, D.S. Neuberg, G. Bollag, M.A. Shipp, and R.C. Aguiar. 2005. The phosphodiesterase PDE4B limits cAMP-associated PI3K/AKT-dependent apoptosis in diffuse large B-cell lymphoma. *Blood*. 105:308–316. doi:10.1182/blood-2004-01-0240

Stall, A.M., M.C. Fariñas, D.M. Tarlinton, P.A. Lalor, L.A. Herzenberg, S. Strober, and L.A. Herzenberg. 1988. Ly-1 B-cell clones similar to human chronic lymphocytic leukemias routinely develop in older normal mice and young autoimmune (New Zealand Black-related) animals. *Proc. Natl. Acad. Sci. USA*. 85:7312–7316. doi:10.1073/pnas.85.19.7312

Stiles, B., M. Groszer, S. Wang, J. Jiao, and H. Wu. 2004. PTENless means more. *Dev. Biol*. 273:175–184. doi:10.1016/j.ydbio.2004.06.008

Suzuki, A., M.T. Yamaguchi, T. Ohteki, T. Sasaki, T. Kaisho, Y. Kimura, R. Yoshida, A. Wakeham, T. Higuchi, M. Fukumoto, et al. 2001. T cell-specific loss of Pten leads to defects in central and peripheral tolerance. *Immunity*. 14:523–534. doi:10.1016/S1074-7613(01)00134-0

Suzuki, A., T. Kaisho, M. Ohishi, M. Tsukio-Yamaguchi, T. Tsubata, P.A. Koni, T. Sasaki, T.W. Mak, and T. Nakano. 2003. Critical roles of Pten in B cell homeostasis and immunoglobulin class switch recombination. *J. Exp. Med*. 197:657–667. doi:10.1084/jem.20021101

Tangye, S.G., V.L. Bryant, A.K. Cuss, and K.L. Good. 2006. BAFF, APRIL and human B cell disorders. *Semin. Immunol*. 18:305–317. doi:10.1016/j.smim.2006.04.004

Uddin, S., A.R. Hussain, A.K. Siraj, P.S. Manogaran, N.A. Al-Jomah, A. Moorji, V. Atizado, F. Al-Dayel, A. Belgaumi, H. El-Solh, et al. 2006. Role of phosphatidylinositol 3′-kinase/AKT pathway in diffuse large B-cell lymphoma survival. *Blood*. 108:4178–4186. doi:10.1182/blood-2006-04-016907

Vazquez, F., and P. Devreotes. 2006. Regulation of PTEN function as a PIP3 gatekeeper through membrane interaction. *Cell Cycle*. 5:1523–1527.

Witzig, T.E., and S.H. Kaufmann. 2006. Inhibition of the phosphatidylinositol 3-kinase/mammalian target of rapamycin pathway in hematologic malignancies. *Curr. Treat. Options Oncol*. 7:285–294. doi:10.1007/s11864-006-0038-1

Yuan, T.L., and L.C. Cantley. 2008. PI3K pathway alterations in cancer: variations on a theme. *Oncogene*. 27:5497–5510. doi:10.1038/onc.2008.245